Genome-wide changes in genetic diversity in a population of *Myotis lucifugus* affected by white-nose syndrome

Lilley TM [1,2], Wilson IW [1], Field KA [3], Reeder DA [3], Turner G [4], Kurta A [5], Blomberg AS [6], Hoff S [7], Herzog C [7], Paterson S [1].

[1]Institute of Integrative Biology, University of Liverpool, United Kingdom. [2]Finnish Museum of Natural History, University of Helsinki, Finland. [3]Biology Department, Bucknell University, 1 Dent Drive, Lewisburg, PA 12837, USA. [4]Pennsylvania Game Commission, Harrisburg, PA, USA. [5]Department of Biology, Eastern Michigan University, Ypsilanti, MI, USA. [6]Department of Biology, University of Turku, Finland. [7]Wildlife Diversity Unit, State Department of Environmental Conservation, Albany, NY, USA.

Corresponding author: tmlill@liverpool.ac.uk

Abstract

Novel pathogens can cause massive declines in populations, but seldom lead to extirpation of hosts. Rather, disease can act as a selective pressure on survivors, driving the evolution of resistance or tolerance. Bat white-nose syndrome (WNS) is a rapidly spreading wildlife disease in North America. The fungus causing the disease invades skin tissues of hibernating bats, resulting in disruption of hibernation behaviour, premature energy depletion, and subsequent death. We use whole-genome sequencing to investigate changes in allele frequencies within a population of *Myotis lucifugus* in eastern North America, to scan for genetic resistance to WNS. Our results show low F_{ST} values within the population across time, i.e. prior to WNS (Pre-WNS) compared to population that has survived WNS (Post-WNS). However, when dividing the population with an arbitrary geographical cut-off between the states of Pennsylvania and New York, a sharp increase in values on scaffold GL429776 is evident in the Post-WNS samples. Genes present in the diverged area are associated with thermoregulation and promotion of brown fat production. Thus, although WNS may not have subjected the entire *M. lucifugus* population to selective pressure, it could allowed the rise of a selection for alleles in Pennsylvania through decreased gene flow within the population, which may contribute to survival. However, the existence of remnant sub-populations in the aftermath of WNS is likely due to multiple factors in bat life history.

Keywords: Opportunistic pathogen, white-nose syndrome, Selective pressure, Genetic resistance.

1. Introduction

The emergence and spread of multiple infectious wildlife diseases during recent decades has had devastating consequences for biodiversity (Daszak et al., 2000; Smith et al., 2006). Unfortunately, for many taxa, anthropogenic activities and climate change appear to be the main causes of exposure to sources of infection (Gallana et al., 2013; Tompkins et al., 2015). With shifting pathogen ranges, disease-related declines in naïve wildlife often threaten the persistence of populations. Examples include chytridiomycosis, which has wiped out populations of amphibians globally (Daszak et al., 1999; Lips et al., 2006), and avian malaria, which caused the sharp decline of island populations of birds (van Riper et al., 1986). More recently, white-nose syndrome (WNS) has been described as one of the most rapidly spreading wildlife diseases ever recorded (Blehert et al., 2009; Frick et al., 2010). Since the discovery of WNS in North America in 2006, ten species of bats have been diagnosed with the disease in 33 U.S. states and 7 Canadian provinces (www.whitenosesyndrome.org, 2019). Genetic evidence suggests that *Pseudogymnoascus destructans*, the causative agent of WNS, was introduced to North America from Europe (Campana et al., 2017; Lorch et al., 2013; Minnis and Lindner, 2013; Ren et al., 2012; Wibbelt et al., 2010), where affected species do not experience associated mortality (Harazim et al., 2018; Puechmaille et al., 2011; Warnecke et al., 2012; Wibbelt et al., 2013; Zukal et al., 2016).

When a disease enters a naïve host population, the initial wave of infection often causes epizootics that result in mass mortality, which may extirpate local host populations or even cause species extinction (Daszak et al., 1999; De Castro and Bolker, 2005; Frick et al., 2010). However, extinctions due to a disease appear to occur seldomly, and a disease can act as a

56 selective pressure on survivors, driving the evolution of tolerance or resistance, which may
57 transform a disease from being epizootic to being enzootic (Boots et al., 2009; Karlsson et al.,
58 2014; Robinson et al., 2012). This may occur through rapid changes in the distribution of
59 genetic variants associated with disease susceptibility over short timescales (Gallana et al.,
60 2013). These powerful selective pressures pathogens exert on naïve host populations (Sironi
61 et al., 2015) and genetic signatures of infection-related selective sweeps may be detectable for
62 generations (Deschamps et al., 2016; Di Gaspero et al., 2012; Groot et al., 2002). Detection of
63 selective sweeps on particular genes or gene families can confirm or exclude potential
64 mechanisms of host susceptibility or pathogen virulence (Campbell and Tishkoff, 2008).
65 Rapid, extreme bottlenecks (such as those caused by panzootic events), meanwhile, are
66 associated with a more stochastic loss of alleles, which does not necessarily indicate selection
67 (Luikart et al., 1998). Much of the research on disease-induced selection has focused on the
68 major histocompatibility complex (MHC), and indeed, diseases can drive the evolution and
69 maintenance of MHC diversity in natural populations (Davy et al., 2017a; Jeffery and
70 Bangham, 2000; Paterson et al., 1998; Spurgin and Richardson, 2010; Teacher Amber G. F. et
71 al., 2009; Zeisset and Beebee, 2014). However, factors not directly associated with interactions
72 between host and pathogen, such as environmental conditions and competition with other
73 species, can have a considerable influence on the manifestation of a disease (Scholthof, 2007).

74 The psychrophilic (cold-growing) fungus *P. destructans*, (Lorch et al., 2011; Minnis and
75 Lindner, 2013; Warnecke et al., 2008) acts as an opportunistic pathogen of bats, invading the
76 skin tissues of hibernating hosts (Cryan et al., 2010; Meteyer et al., 2012). Susceptible species,
77 such as *M. lucifugus* and *M. septentrionalis*, have shown population declines greater than 90%
78 in affected hibernacula (Frick et al., 2015). The infection disrupts the hibernation behaviour of

79 the bats and leads to more frequent arousals from torpor, evaporative water loss, premature
80 energy depletion, and death of susceptible individuals due to emaciation (McGuire et al., 2017;
81 Reeder et al., 2012; Verant et al., 2014; Warnecke et al., 2013; Willis et al., 2011). Naïve
82 infected *M. lucifugus* upregulate genes involved in immune pathways during hibernation (Davy
83 et al., 2017b; Field et al., 2015, 2018; Lilley et al., 2017). These responses are weak during
84 torpor but are robust after arousal, supporting the hypothesis that periodic arousals are
85 necessary to initiate immune responses to pathogens or to augment responses that occur at low
86 levels during torpor (Field et al., 2018; Luis and Hudson, 2006). Therefore, increased arousals
87 may be attempts by the host to fight off the pathogen, in addition to quenching thirst, expelling
88 waste and possibly foraging (Bernard and McCracken, 2017; Willis et al., 2011) and
89 supplementing electrolytes (Cryan et al., 2013). White-nose syndrome is a prime example of a
90 disease which is manifested when factors associated with the environment (i.e. temperature
91 and humidity of the hibernaculum), the host (and the host's response to infection) and the
92 pathogen correlate favourably (Scholthof, 2007). Therefore bat species, and populations within
93 species, are affected differently according to hibernation behaviour and prevailing micro-
94 climate conditions in available hibernacula (Grieneisen et al., 2015; Johnson et al., 2014;
95 Langwig et al., 2015). As such, with a wildlife disease dependent on outside host interactions,
96 such as WNS, loci not associated with MHC diversity or other immune response-associated
97 factors, such as the amount of body fat prior to hibernation (Cheng et al., 2019), may also affect
98 survival of species and populations. This highlights the importance of examining the genome
99 as a whole (Sparks et al., 2019).

100 The initial impacts of WNS on six species of hibernating bats in the northeastern and
101 midwestern USA vary from almost complete extirpation to arrested population growth (Turner

102 et al., 2011). After the initial decline caused by WNS in *M. lucifugus*, reports have surfaced
103 describing stabilisation at smaller sizes or even increases in numbers of individuals (Dobony
104 and Johnson, 2018; Frick et al., 2017; Langwig et al., 2015; Maslo et al., 2015). Models
105 parameterised with long-term data on fungal loads, infection intensity and counts of bats at
106 hibernacula have suggested development of either tolerance or resistance in these persisting
107 populations (Frick et al., 2017), which is supported by reports on infected bats not arousing
108 from torpor as frequently as during the acute phase of the zoonosis (Lilley et al., 2016). Since
109 WNS has inflicted massive population declines in some species, there is a possibility that
110 selection could occur for alleles conferring resistance or tolerance from the standing genetic
111 variation, which would confer to resistance or tolerance could occur. Indeed, Maslo and
112 Feffermann (2015) suggested the occurrence of evolutionary rescue occurring and Donaldson
113 et al. (2017) described changes in an immunome across *M. lucifugus* populations obtained
114 through a sequence capture method, which may be attributed to selection by WNS. A study
115 suggests the initially affected *M. lucifugus* population is beginning to show signs of resistance
116 to the pathogen (Langwig et al., 2017). However, the possible selective pressures WNS has
117 exerted on the population, which may not even be related to immune responses (e.g. Cheng et
118 al., 2019), are yet to be described at the whole-genome level using high-depth sequencing depth
119 (although see Gignoux-Wolfsohn et al., 2018).

120 Here, we utilise high-throughput whole-genome sequencing on the WNS-affected species *M.*
121 *lucifugus*, allowing us to look at entire genomes via single nucleotide polymorphisms (SNPs).
122 We compare genetic patterns (F_{ST} and heterozygosity) before and after the spread of WNS in
123 the eastern North American population to gain insight into whether the disease is causing
124 selection of major loci in surviving bats. We hypothesise that, due to the massive population

125 declines caused by WNS and the fact that the affected population is now beginning to stabilise
126 or slightly increase in size (Langwig et al., 2017), a soft selective sweep based on standing
127 genetic variation has resulted in differentiation in one or many regions of the genome (Messer
128 and Petrov, 2013). Adaptation could therefore be in the process of driving the evolutionary
129 rescue of a population, in which individuals resistant or tolerant to the disease survived a
130 bottleneck and passed these traits to their offspring (Carlson et al., 2014). Alternatively,
131 survival may be due to factors not related to selection for WNS-resistant alleles, such as
132 microbiome adaptation (Ange-Stark et al., 2019; Lemieux-Labonté et al., 2017) or stochasticity
133 in hibernation site microhabitat. This study provides a foundation for future work on genome-
134 wide effects of WNS in *M. lucifugus* and other affected species of bats.

135 2. Materials and methods

136 2.1. Ethics Statement

137 This study was carried out on bats from non-endangered species in strict accordance with
138 recommendations in the Guide for the Care and Use of Laboratory Animals of the National
139 Institutes of Health. All methods were approved by the Institutional Animal Care and Use
140 Committee at Bucknell University (protocol DMR-016). The bats were collected under
141 Pennsylvania Game Commission Special Use Permit #33085, and New York State Department
142 of Environmental Conservation Permit #427.

143 2.2. Sample collection and DNA extraction

144 We conducted whole-genome sequencing on a population of *M. lucifugus* prior to, and up to
145 10 years after, the onset of WNS. White-nose syndrome in bats was first observed in upstate

146 New York, at Howe's Cave during the winter of 2006-2007 (Blehert et al., 2009). Our historic
147 samples were obtained from individuals consisting of the eastern population of *M. lucifugus*
148 (Miller-Butterworth et al., 2014; Vonhof et al., 2015) from New York (NY) (from the first
149 batch of dead bats found at Howe's Cave in 2006) and from bats caught in central Pennsylvania
150 (PA) in 2005-2006 (Table 1.,Supp. Table 1.). Bats in PA became affected by the disease in
151 roughly 2008–2009. The remnants of the eastern North American population in NY and PA
152 were sampled again in 2016, and genetic diversity was compared before and after WNS (Table
153 1., Supp. Table 1.). We sampled wing tissue from frozen specimens of known origin (Supp.
154 Table 1.) that were collected and stored by the New York State Department of Environmental
155 Conservation (Delmar, NY) and D. Reeder to obtain Pre-WNS samples. Post-WNS bats were
156 captured using mist nets and harp traps during 2015 -2016. In addition to samples from PA and
157 NY, we also collected two samples from Upper-Peninsula Michigan (UPMI) for polymorphic
158 site selection (see Section 2.3.) to increase the diversity of sites for our samples. Tissue samples
159 were collected using either 3.0 mm or 5.0 mm biopsy punches (Integra Milltex, Plainsboro,
160 NJ) and stored in 95% ethanol until extraction. We extracted DNA using QIAmp DNA Mini
161 Kits (Qiagen, Hilden Germany) and stored DNA at -80°C until sequencing.

162 ## 2.3. Sequencing methods

163 Sequencing libraries were made for two sets of data: (1) Six individuals from PA (N = 2), NY
164 (N = 2) and UPMI (N= 2) in order to initially identify a set of polymorphic sites within the *M.*
165 *lucifugus* genome within the focal population (See Supp. Table 1. for information on
166 individuals). Individual sequencing increases the confidence of SNP discovery, relative to
167 pooled sequencing, since individuals exhibit discrete variation in the number of alleles they

168 carry at each potential SNP site; (2) Equimolar pools of DNA from multiple individuals from
169 within our north-eastern US population (NY and PA) at each of two timepoints (pre- and post-
170 WNS) to give four pooled sequencing libraries. TruSeq Nano libraries with a 350 bp insert size
171 were prepared from all samples and run on a HiSeq4000 platform to generate 2x 150 bp reads
172 providing ~15 Gbp of sequence data (~7.5x coverage) for each individual and ~90 Gbp of
173 sequence data (~45x coverage) for each pool. Adapter sequences were removed with Cutadapt
174 v1.2.1 and trimmed with Sickle 1.200 with a minimum quality score of 20.

175 ## 2.4. Bioinformatics methods

176 Reads from the six individuals were mapped onto the *M. lucifugus* reference genome
177 (https://www.broadinstitute.org/brown-bat/little-brown-bat-genome-project) using Bowtie2
178 v2.2.5 (Langmead and Salzberg, 2012), with the '—sensitive-local' preset. Reads were sorted
179 using SAMtools v1.1 (Li et al., 2009) and combined by read group (with duplicates removed
180 using a 'lenient' validation stringency setting) using Picard-tools v2.5.0
181 (http://broadinstitute.github.io/picard). SNPs were called across all six individuals with the
182 Genome Analysis Toolkit (GATK) v3.4 HaplotypeCaller (McKenna et al., 2010) using default
183 parameters. Within this SNP set, high-quality bivalent SNPs were selected that met selection
184 criteria across the six individuals (Quality Score > 100; AF<1; 30>=DP>=100) and were input
185 to the SAMtools mpileup function as a list of sites at which pileup was to be generated.

186 Reads from the pooled samples were mapped to the *M. lucifugus* reference genome as above
187 and SAMtools mpileup was used to count alleles at high-quality SNP sites identified above
188 (i.e. reads matching either the reference or alternate allele for bivalent loci). Sites with coverage
189 in the bottom 10% or top 10% quantiles summed across the pooled samples were excluded

190 (since these could reflect inaccuracies in the reference genome), leaving about 13.5 million
191 sites.

192 Average heterozygosity within the pooled samples was calculated using npstats (Ferretti et al.,
193 2013), which controls for number of individuals within each sequencing pool and sequencing
194 depth, thus allowing robust comparisons between pooled samples. One million SNPs were
195 randomly picked and permuted, with 1000 sets of 1000 SNPs used to calculate the observed
196 heterozygosity within each pooled set of individuals and, from these, we produced the median
197 and 95% confidence intervals on heterozygosity.

198 Using allele counts at each locus to estimate allele frequencies, F_{ST} was calculated without
199 weighting for sampling effort ($F_{ST} = \left(\bar{p}(1-\bar{p}) - \overline{p(1-p)}\right)/\bar{p}(1-\bar{p})$, where p is the allele
200 frequency and either averaged between populations ($\bar{p}$) or the value $p(1-p)$ averaged across
201 populations). F_{ST} was separately calculated between the Pre-WNS and Post-WNS samples and
202 between subsections thereof, specifically PA pre- vs post-WNS, NY pre- vs post-WNS, PA
203 pre- vs NY pre-WNS, PA post- vs NY post-WNS, and all PA vs all NY). Selection is expected
204 to elevate F_{ST} at specific genomic regions relative to background levels due to sampling noise
205 or genetic drift, which are expected to act equally across the genome. To identify such regions
206 across the genome, a moving window was applied to calculate median pairwise F_{ST} values for
207 groups of 500 consecutive SNPs at a time to even out sampling effects. Moving windows
208 shifted 100 SNPs at a time, thus providing the best balance between fine detail and practicality.
209 Allele frequency estimates were weighted by the number of individuals in each pool. This was
210 done using a custom R script (see Data availability section), run using R v3.4.1 (R
211 Development Core Team, 2011). Results were confirmed using Popoolation2 with a 10 kb

212 sliding window and with defined pool sizes. This gave the same qualitative results, but higher
213 levels of background noise (Kofler et al., 2011). Additionally, Popoolation2 was used to
214 perform Fishers Exact Tests on individual SNPs in order to test whether any very highly
215 significant SNPs were missed by the moving window approach.

216 From the comparison of the NY and PA pooled samples (i.e. the comparison that produced the
217 highest F_{ST} values), we visually identified across the whole genome windows with median F_{ST}
218 values greater than 5 standard deviations from the mean, as well as those with F_{ST} values greater
219 than 0.05, indicating at least 'moderate' genetic differentiation (Wright, 1978). The numbers
220 of such complete windows within gene models were counted for each gene to identify genes
221 potentially under selective pressure.

222 3. Results

223 3.1. Pre-WNS vs Post-WNS comparisons

224 To detect regions of the genome that may be under selection, we plotted F_{ST} across the *M.*
225 *lucifugus* genome, calculated from allele counts within moving windows covering 500 SNPs
226 and shifting 100 SNPs at a time. Comparing Pre- and Post-WNS samples revealed an overall
227 low level of population differentiation due to genetic structure (F_{ST} median of 0.0059; Table
228 2). Whilst a small number of windows have F_{ST} values slightly beyond our arbitrary cut-off of
229 5 standard deviations above the mean, none have F_{ST} values exceeding 0.05, suggesting that
230 there is not even moderate selection in any region of the genome in Post-WNS samples
231 compared to Pre-WNS samples (Fig. 2, Table 2)(Wright, 1978). Similarly, using Fisher exact
232 tests from Popoolation2 at a threshold of $p < 10^{-6}$, no individual SNPs were found to be
233 consistently associated with differences Pre- versus Post-WNS among the four sets of samples.

234 ### 3.2. Comparisons within US states

235 Due to our sampling and sequencing setup, we were also able to separately look at individuals
236 of the same population from two discrete geographical locations within their range. In our case
237 an arbitrary divide was made between bats sampled in NY and PA. Although population
238 genetic analysis based on a considerably lower number of genetic markers assigns *M. lucifugus*
239 on the eastern coast of North America to the same population (Vonhof et al., 2015), the species
240 shows high degrees of philopatry (Davis and Hitchcock, 1965; Norquay et al., 2013),
241 warranting the examination of these arbitrarily assigned pools of individuals outside the mean
242 dispersal range of the species using more accurate, whole-genome sequencing based population
243 genetic analyses.

244 A number of minor differences (F_{ST} > 5 stdevs above mean, but F_{ST} < 0.05) between these
245 arbitrary sets of samples are evident prior to arrival of WNS, as well as a peak in scaffold
246 GL429835 with an F_{ST} value exceeding 0.05 (Fig. 3a). The high peak consists of 4 windows
247 the midpoints of which span an 81,887 bp region within a coding sequence consisting of 47
248 exons, which encodes the NIPBL cohesion loading factor (NCBI Gene ID: 102430106). The
249 highest peak in a comparison of PA populations Pre- and Post-WNS (Fig. 3b) lies in a similar
250 position within this coding region, as does a peak in a similar comparison of NY samples (Fig.
251 3c), though neither exceed the F_{ST} value cut-off of 0.05.

252 ### 3.3. Post-WNS comparisons between US states

253 When comparing the Post-WNS individuals sampled from PA with the Post-WNS individuals
254 from NY, the peak on scaffold GL429835 is no longer visible, but a far more pronounced spike

255 in F_{ST} values can be clearly seen in scaffold GL429776 (Fig. 4a), indicating relatively large
256 allele frequency differences between the sample sets in this region of the genome. This is also
257 seen, to a lesser extent, when comparing all samples from NY with all samples from PA (Fig.
258 4b). However, this significant peak in this comparison of all samples collected does not affect
259 average fixation across the genome relative to the other comparison of all samples, Pre-WNS
260 vs Post-WNS (Table 2).

261 We examined scaffold GL429776 more closely to compare the F_{ST} values between individuals
262 from the arbitrarily selected sample sets from NY Post-WNS and PA Post-WNS (Fig. 4a).
263 Genes within scaffold GL429776 containing windows with fixation values > 0.05 between the
264 NY Post-WNS and PA Post-WNS samples, are presented in Table 4 and Fig. 4a.

265 To clarify why we saw no fixation at this site when comparing Pre-WNS and Post-WNS
266 populations (Fig. 3a), nor when we compared Pre-WNS samples from both geographical
267 origins (Figs. 3b and 3c), we calculated for the relevant subpopulations the proportion of
268 reference alleles called at each site included in the F_{ST} window analyses (Fig. 5). This revealed
269 a small decrease over time in the proportion of the reference alleles seen at this locus in the PA
270 subpopulation (Fig. 5a), commensurate with an increase in proportion of reference alleles in
271 the NY sample set (Fig. 5b). As such, existing differences between the NY and PA sample sets
272 were insufficient to cause a relative rise in fixation prior to WNS spreading through the
273 population (Fig 5c). Conversely, Post-WNS, allele proportions at this site in both sample sets
274 had not changed sufficiently to suggest selection *within* the sample set but demonstrated clear
275 differences *between* the NY and PA sample sets (Fig. 5d).

276 In the Post-WNS comparison, peaks which were above our arbitrary threshold of 5 standard
277 deviations above the mean across the whole genome, but below F_{ST} = 0.05, can also be
278 observed in small scaffolds on the right-hand side of the F_{ST} plots. The 63 windows comprising
279 these peaks lie in 47 scaffolds. Of these, high F_{ST} windows lie in only 6 protein-coding regions
280 across 6 scaffolds (Table 3). Two of these encode partial gene models. Of the 4 remaining
281 models containing high F_{ST} regions, all but 1 is described on NCBI as a "Low Quality Protein".
282 The exception is a gene encoding the ankyrin 2 protein, within which 7 high F_{ST} windows lie.

283 ### 3.4. Measures of heterozygosity within subpopulations

284 We examined heterozygosity across the genome in the subpopulations divided by time and
285 location to measure whether the epizootic reduces genetic diversity. We found the following
286 values: PA pre-WNS: Median: 0.263 (0.252 – 0.274 95% CI); PA post-WNS: 0.247 (0.239 –
287 0.255); NY pre-WNS: 0.255 (0.247 – 0.263); and NY post-WNS: 0.256 (0.247 -0.265).

288 ## 4. Discussion

289 Examining our data as a whole, we found low F_{ST} values between the Pre- and Post-WNS
290 individuals of our eastern North American *M. lucifugus* population, the absence of fixation
291 suggesting that WNS has not decreased the population in size sufficiently for the disease to
292 have an effect on genetic diversity. Also, we found no significant changes in within-population
293 heterozygosity Post-WNS, despite the massive population declines caused by WNS over the
294 past decade, and found overall high heterozygosity across the genome. These results are in
295 accordance with a similar, low-coverage study conducted by Gignoux-Wolfsohn et al. (2018).
296 Panmixia of populations in evolutionary time in bats to the east of the Rocky Mountains has

297 been previously documented (Vonhof et al., 2016; Wilder et al., 2015). Gignoux-Wolfsohn *et*
298 *al.* (2018) present evidence for a soft selective sweep, where selection acts on standing genetic
299 variation, between Pre- and Post-WNS populations. Their analysis is based on a change in
300 minor allele frequencies due to selection, distinguished from background demography using a
301 simulation approach; and it shows a complex picture of potentially up to 85 unlinked SNPs,
302 each exhibiting small effects and with little or no selective signal at adjacent SNPs. In contrast,
303 a recent case study of selection on standing genetic variation, by myxoma virus in rabbits,
304 showed that soft selective sweeps caused concerted changes in allele frequencies at sets of
305 linked SNPs around coding loci (Alves et al., 2019).

306 The species originally described as *M. lucifugus* in North America (Fenton and Barclay, 1980)
307 has since been divided into five non-sister species (Morales and Carstens, 2018). All of the
308 individuals sampled in our study belong to *M. lucifugus senso stricto*, with a range extending
309 from the east coast of North America to Alaska, and furthermore, to the same previously
310 assigned population (Miller-Butterworth et al., 2014). Previous nuclear genetic studies show
311 that differentiation is low, and there is no evidence for any major barriers to nuclear gene flow
312 across the range of *M. lucifugus*.

313 Due to our sampling design, we were able to separate bats geographically within our sampling
314 range. We made the arbitrary cut-off point for a more in-depth investigation of bats sampled in
315 the states of PA compared to NY. Here, we see low F_{ST} values between the two groups of bats
316 prior to the onset of WNS, indicating an absence of selection across the genome, with the
317 exception of a small peak in scaffold GL429835, which lies within a gene model encoding the
318 NIPBL cohesion loading factor. Relatively high F_{ST} values are also visible within this region

319 when comparing the PA population before and after the spread of WNS, as well as the NY
320 population pre- and post-WNS. However, this peak is not evident when comparing PA and NY
321 post-WNS (Fig. 4a). This suggests that this coding sequence was under selective pressures,
322 manifesting as different allelic fixations, in both subpopulations prior to the arrival of WNS,
323 but that any selection was nullified by the population-level impact of WNS (or another event
324 occurring during the same timeframe). The protein NIPBL, as described in a review by Peters
325 et al. (2008) plays an important role in the function of the cohesin complex, which is vital for
326 chromosome segregation, DNA damage repair, and gene expression regulation. As these
327 results suggest the loss of low-level functional diversity at this locus in our subpopulations, it
328 would be interesting to further investigate what impact this will have on the population as a
329 whole.

330 The F_{ST} comparison of Post-WNS individuals sampled from PA and NY depicts considerable
331 genetic differentiation within scaffold GL429776; differentiation which did not exist in the
332 Pre-WNS comparison of individuals sampled from these geographical areas. This is a
333 difference which would have gone unnoticed had we not made the arbitrary comparison
334 between bats sampled in NY and PA, or used fewer genetic markers instead of a whole-genome
335 approach (Miller-Butterworth et al., 2014; Vonhof et al., 2015). The region's appearance post-
336 WNS when considering all geographical locations together is not, however, reflected when the
337 data are broken down into representatives of each state. A comparison of allele frequencies of
338 individual SNPs within this region shows that individuals sampled from PA showed an increase
339 in deviation from the reference genome over time, whilst a greater proportion of reference
340 alleles were seen in NY samples Post-WNS compared with Pre-WNS. The differences in

341 proportions, growing as they were over time, were insufficient to exhibit a high fixation value
342 Pre-WNS, but were notably different after the disease had spread through the population.

343 This region within the scaffold containing the peak contains six annotated genes with very
344 different functions. Two, POC1B and CEP290, are involved in cilia development and
345 maintenance. The ATP2B1 gene encodes a protein which belongs to the family of P-type
346 primary ion transport ATPases, whereas TMTC3 is involved in the control of endoplasmic
347 reticulum stress response. MGAT4C is a glycosyltransferase that participates in the transfer of
348 N-acetylglucosamine (GlcNAc) to the core mannose residues of N-linked glycans. Finally,
349 KITLG produces a protein involved in mast cell development, migration and function, and
350 melanogenesis. KITLG has been documented as a target of evolution in recent studies and in
351 humans it has been linked with thermoregulation (Yang et al., 2018), which is a critical
352 component of bat life history (Studier and O'Farrell, 1972). In fact, upregulation of KITLG at
353 low temperature helps promote the production of brown fat for heat generation (Huang et al.,
354 2014). Bats utilise brown adipose tissue in arousals to normothermia from different degrees of
355 torpor (Thomas et al., 1990). There is also evidence of parallel evolution of pigmentation in
356 sticklebacks and humans linked to KITLG (Miller et al., 2007), as well as its role in determining
357 resistance/susceptibility to swine respiratory diseases in Erhulian pigs (Huang et al., 2017).
358 KITLG, by influencing mast cell development, could also play a role in either protective or
359 pathological immune responses to *P. destructans*, which may involve IgE-mediated
360 recognition of secreted fungal proteins. As such, temporal changes we found in allele
361 frequencies at this locus could, for instance, be linked to differences in hibernation site
362 temperatures, and/or thermoregulatory needs in bats sampled at different locations (Humphries
363 et al., 2002; Thomas et al., 1990). Spatial patterns, as seen here between the arbitrarily pooled

364 samples from PA and NY, could be due to local adaptation, in which strong selective sweeps
365 may be linked to gene variants favoured in local interactions (Hansen et al., 2012; Kyle et al.,
366 2014; Rico et al., 2015; Schoville et al., 2012). Whilst we lack data concerning migration
367 patterns of the bats studied here, as well as the environmental conditions within their
368 microfugia, future work would benefit from these data in a bid to understand whether bats
369 repeatedly frequent habitats with similar conditions and whether, indeed, there is a significant
370 difference in conditions across these Eastern states that explains the rapid rise in fixation at this
371 locus.

372 The increase in F_{ST} values in this scaffold GL429776 could, alternatively, be due to the massive
373 population decline caused by WNS (Langwig et al., 2017). Although not supported by existing
374 data, the decline could potentially have resulted in a decrease in connectivity and gene flow
375 between remnant local populations allowing for a local adaptation to arise (Bohonak, 1999;
376 Lilley, Anttila, & Ruokolainen, 2018). Genetically resolved examples of local adaptations are
377 rare (Hoekstra et al., 2006) and, in our focal system, pinpointing the causality leading to local
378 adaptation is especially difficult due to the cryptic life history of bats. Determining how these
379 variants are spread or localised among populations is essential to understanding and managing
380 the emergence of new selective pressures (Eizaguirre et al., 2012; Kyle et al., 2014). We cannot
381 fully exclude the possibility of WNS selecting for alleles in our scaffold of interest through. It
382 is likely that there is concurrent selection occurring across multiple populations, and that
383 selection is not acting to the same degree or even on the same loci in different geographic areas
384 affected by WNS (Messer and Petrov, 2013). This also applies to interpreting the results on a
385 smaller scale: the samples had not been collected from exactly the same locations before and
386 after WNS, which may contribute to our results. Individuals sampled during the winter, at their

387 hibernacula, may not inhabit the vicinity of these locations during the summer, although
388 dispersal distances are often short (Davis & Hitchcock, 1965; but see Norquay et al., 2013).
389 Understanding how local separate sub-populations cope with pathogen pressure would benefit
390 from an RNAseq-approach identifying responses at transcript-level (Lilley et al., 2019).

391 The ankyrin 2 protein encoding gene, lying within the observed small scaffolds on the right-
392 hand side of the F_{ST} plots has a wide range of attributed Gene Ontology functions (The UniProt
393 Consortium, 2019), which reinforce the ubiquitous nature and far-reaching roles of ankyrin-
394 repeat-containing genes across organisms (Voronin and Kiseleva, 2007). Alternatively, the
395 peaks in this area may have arisen because only relatively few SNPs were called there given
396 the small size of the scaffolds, thus limiting our ability to generate high-quality windows, hence
397 the greater sampling noise.

398 Despite not seeing an overarching genetic signal associated with resistance in *M. lucifugus*,
399 remnant populations appear to be surviving year after year and even increasing in size
400 notwithstanding infection loads during the hibernation period (Langwig et al., 2017; Lilley et
401 al., 2016). The fact that the intensity of infection with *P. destructans* appears to be significantly
402 lower for remnant populations compared to colonies in the midst of the epidemic phase and
403 massive declines may suggest the development of resistance in these populations (Bernard et
404 al., 2017; Langwig et al., 2017; but see Lilley et al., 2019). However, the role of environmental
405 interactions during the hibernation period, when the bat hosts are most vulnerable to the
406 pathogen, have been largely neglected, although the effect of humidity and temperature on the
407 growth of the fungal pathogen and survival of the host have been separately studied (Grieneisen
408 et al., 2015; Marroquin et al., 2017; Verant et al., 2012). Modelling also suggests that

409 environmental factors, including the cave microbiome, have an impact on the proliferation and
410 infectivity of *P. destructans* (Hayman, Pulliam, Marshall, Cryan, & Webb, 2016; Lilley et al.,
411 2018). This is supported by the discovery of microbes in hibernacula environments and bats
412 that are able to retard the growth of the fungus (Micalizzi et al., 2017; Zhang et al., 2014, 2015).
413 In light of our results and considering bat life history as a whole, adaptation and evolutionary
414 rescue may not be a fast track for recovery of bat populations affected by WNS (Maslo and
415 Fefferman, 2015), although ultimately these will contribute to long term survival of populations
416 (Lilley et al., 2019). At the present, it is more likely the variability in hibernation site
417 environmental conditions and strong selection for microbial taxa that inhibit *P. destructans*
418 could explain why populations are recovering from the zoonosis (Cheng et al., 2016; Lemieux-
419 Labonté, Simard, Willis, & Lapointe, 2017; Lilley et al., 2018).

420 It is still unclear how frequently genetic adaptation occurs in natural populations and under
421 what circumstances it is promoted (Schoville et al., 2012). Many studies have recorded
422 phenotypic changes in natural populations and attributed them to host-pathogen interactions
423 (Frank et al., 2014; Kilpatrick, 2006; Langwig et al., 2017; Råberg et al., 2009). However, it is
424 difficult to determine conclusively whether changes in phenotype are the result of selection in
425 the genome or a result of phenotypic plasticity (Paterson et al., 2010; Routtu and Ebert, 2015).
426 Also, the assumed benefit of change (i.e. adaptation) is often not tested experimentally, which
427 would allow for inference of causality with the pathogen through exclusion of other potential
428 drivers.

429 To conclude, our results suggest WNS has not yet decidedly subjected populations of *M.*
430 *lucifugus* to selective pressures leading to genetic adaptation in remnant populations. No

431 population -wide signs of selection in comparisons of genomes of Pre-WNS and ten years Post-
432 WNS populations were observed (but see Donaldson et al., 2017; Gignoux-Wolfsohn et al.,
433 2018). This is something that is not unexpected with a species in which the effective population
434 size most likely numbered in tens of millions of individuals prior to the onset of WNS. Our
435 results indicate that the existence and recent growth of remnant populations of *M. lucifugus* are
436 more likely attributable to other factors, such as microbiome adaptation and hibernation site
437 selection among others, rather than genetic adaption. However, we found increased variability
438 in a specific area of the genome in a comparison of Post-WNS samples from our two different
439 study states, relative to Pre-WNS samples. We suggest this is due to weakened connectivity
440 between bats at different locations allowing for local adaptations to enrich in the absence of
441 gene flow. Although genes in the high F_{ST} region of the genome were identified, and genes
442 such as KITLG provide interesting avenues of research, even with regards to WNS, further
443 investigation into the processes in bat life history to which these genes are related are required
444 to expound upon the existing gene annotations.

445 ## Acknowledgements

446 We thank Svenska Kulturfonden, H2020 Marie Skłodowska-Curie Actions (TML, 706196)
447 and the Natural Environment Research Council, UK for funding the study; staff at the Centre
448 for Genomic Research, University of Liverpool, UK for DNA sequencing expertise; Jenni
449 Prokkola and Riley F. Bernard for proofreading the manuscript; and Alice Lilley, Cali Wilson,
450 Beth Rogers and Mike Scafini for assisting in sample collection.

Author contributions

TML and SP designed the research. TML, DMR, KAF, AK, GGR and CH collected the samples. TML prepared samples for sequencing. TML, IWW and SP analysed the data. TML, IWW and SP wrote the first draft of the manuscript, and all authors contributed to the final version.

Data availability statement

Raw data are available at ENA accession XXXXX and bioinformatics code at https://github.com/scottishwormboy/myoluc.

References

Alves, J.M., Carneiro, M., Cheng, J.Y., Matos, A.L. de, Rahman, M.M., Loog, L., Campos, P.F., Wales, N., Eriksson, A., Manica, A., et al. (2019). Parallel adaptation of rabbit populations to myxoma virus. Science *363*, 1319–1326.

Ange-Stark, M., Cheng, T.L., Hoyt, J.R., Langwig, K.E., Parise, K.L., Frick, W.F., Kilpatrick, A.M., MacManes, M.D., and Foster, J.T. (2019). White-nose syndrome restructures bat skin microbiomes. BioRxiv 614842.

Bernard, R.F., and McCracken, G.F. (2017). Winter behavior of bats and the progression of white-nose syndrome in the southeastern United States. Ecol. Evol. *7*, 1487–1496.

Bernard, R.F., Willcox, E.V., Parise, K.L., Foster, J.T., and McCracken, G.F. (2017). White-nose syndrome fungus, Pseudogymnoascus destructans, on bats captured emerging from caves during winter in the southeastern United States. BMC Zool. *2*, 12.

471 Blehert, D.S., Hicks, A.C., Behr, M., Meteyer, C.U., Berlowski-Zier, B.M., Buckles, E.L.,
472 Coleman, J.T.H., Darling, S.R., Gargas, A., Niver, R., et al. (2009). Bat white-nose syndrome:
473 an emerging fungal pathogen? Science *323*, 227–227.

474 Bohonak, A.J. (1999). Dispersal, gene flow, and population structure. Q. Rev. Biol. *74*, 21–45.

475 Boots, M., Best, A., Miller, M.R., and White, A. (2009). The role of ecological feedbacks in
476 the evolution of host defence: what does theory tell us? Philos. Trans. R. Soc. Lond. B Biol.
477 Sci. *364*, 27–36.

478 Campana, M., Kurata, N., Foster, J.T., Helgen, L., Reeder, D., Fleischer, R., and Helgen, K.M.
479 (2017). White-nose syndrome fungus in a 1918 bat specimen from France. Emerg. Infect. Dis.
480 J. *23*, 1–1.

481 Campbell, M.C., and Tishkoff, S.A. (2008). African Genetic Diversity: Implications for
482 Human Demographic History, Modern Human Origins, and Complex Disease Mapping. Annu.
483 Rev. Genomics Hum. Genet. *9*, 403–433.

484 Carlson, S.M., Cunningham, C.J., and Westley, P.A.H. (2014). Evolutionary rescue in a
485 changing world. Trends Ecol. Evol. *29*, 521–530.

486 Cheng, T.L., Mayberry, H., McGuire, L.P., Hoyt, J.R., Langwig, K.E., Nguyen, H., Parise,
487 K.L., Foster, J.T., Willis, C.K.R., Kilpatrick, A.M., et al. (2016). Efficacy of a probiotic
488 bacterium to treat bats affected by the disease white-nose syndrome. J. Appl. Ecol. *54*, 701–
489 708.

490 Cheng, T.L., Gerson, A., Moore, M.S., Reichard, J.D., DeSimone, J., Willis, C.K.R., Frick,
491 W.F., and Kilpatrick, A.M. (2019). Higher fat stores contribute to persistence of little brown
492 bat populations with white-nose syndrome. J. Anim. Ecol. *0*.

493 Cryan, P.M., Meteyer, C.U., Boyles, J.G., and Blehert, D.S. (2010). Wing pathology of white-
494 nose syndrome in bats suggests life-threatening disruption of physiology. Bmc Biol. *8*, 135.

495 Cryan, P.M., Meteyer, C.U., Blehert, D.S., Lorch, J.M., Reeder, D.M., Turner, G.G., Webb, J.,
496 Behr, M., Verant, M., Russe, R.E., et al. (2013). Electrolyte depletion in white-nose syndrome
497 bats. J. Wildl. Dis. *49*, 398–402.

498 Daszak, P., Berger, L., Cunningham, A.A., Hyatt, A.D., Green, D.E., and Speare, R. (1999).
499 Emerging infectious diseases and amphibian population declines. Emerg. Infect. Dis. *5*, 735–
500 748.

501 Daszak, P., Cunningham, A.A., and Hyatt, A.D. (2000). Emerging infectious diseases of
502 wildlife-threats to biodiversity and human health. Science *287*, 443–449.

503 Davis, W.H., and Hitchcock, H.B. (1965). Biology and migration of the bat, *Myotis lucifugus*,
504 in New England. J. Mammal. *46*, 296–313.

505 Davy, C.M., Donaldson, M.E., Rico, Y., Lausen, C.L., Dogantzis, K., Ritchie, K., Willis,
506 C.K.R., Burles, D.W., Jung, T.S., McBurney, S., et al. (2017a). Prelude to a panzootic: Gene
507 flow and immunogenetic variation in northern little brown myotis vulnerable to bat white-nose
508 syndrome. FACETS.

509 Davy, C.M., Donaldson, M.E., Willis, C.K.R., Saville, B.J., McGuire, L.P., Mayberry, H.,
510 Wilcox, A., Wibbelt, G., Misra, V., Bollinger, T., et al. (2017b). The other white-nose
511 syndrome transcriptome: Tolerant and susceptible hosts respond differently to the pathogen
512 Pseudogymnoascus destructans. Ecol. Evol. 7161–7170.

513 De Castro, F., and Bolker, B. (2005). Mechanisms of disease-induced extinction. Ecol. Lett. *8*,
514 117–126.

515 Deschamps, M., Laval, G., Fagny, M., Itan, Y., Abel, L., Casanova, J.-L., Patin, E., and
516 Quintana-Murci, L. (2016). Genomic Signatures of Selective Pressures and Introgression from
517 Archaic Hominins at Human Innate Immunity Genes. Am. J. Hum. Genet. *98*, 5–21.

518 Di Gaspero, G., Copetti, D., Coleman, C., Castellarin, S.D., Eibach, R., Kozma, P., Lacombe,
519 T., Gambetta, G., Zvyagin, A., Cindrić, P., et al. (2012). Selective sweep at the Rpv3 locus
520 during grapevine breeding for downy mildew resistance. TAG Theor. Appl. Genet. Theor.
521 Angew. Genet. *124*, 277–286.

522 Dobony, C.A., and Johnson, J.B. (2018). Observed resiliency of little brown myotis to long-
523 term white-nose syndrome exposure. J. Fish Wildl. Manag. *9*, 168–179.

524 Donaldson, M.E., Davy, C.M., Willis, C.K.R., McBurney, S., Park, A., and Kyle, C.J. (2017).
525 Profiling the immunome of little brown myotis provides a yardstick for measuring the genetic
526 response to white-nose syndrome. Evol. Appl. *10*, 1076–1090.

527 Eizaguirre, C., Lenz, T.L., Kalbe, M., and Milinski, M. (2012). Divergent selection on locally
528 adapted major histocompatibility complex immune genes experimentally proven in the field.
529 Ecol. Lett. *15*, 723–731.

530 Fenton, M.B., and Barclay, R.M.R. (1980). *Myotis lucifugus*. Mamm. Species 1–8.

531 Ferretti, L., Ramos-Onsins, S.E., and Pérez-Enciso, M. (2013). Population genomics from pool
532 sequencing. Mol. Ecol. *22*, 5561–5576.

533 Field, K.A., Johnson, J., Lilley, T., Reeder, S., Rogers, E., Behr, M., and Reeder, D. (2015).
534 The white-nose syndrome transcriptome: activation of anti-fungal host responses in wing tissue
535 of hibernating bats. Plos Pathog. *11*, e1005168.

536 Field, K.A., Sewall, B.J., Prokkola, J.M., Turner, G.G., Gagnon, M., Lilley, T.M., White, J.P.,
537 Johnson, J.S., Hauer, C.L., and Reeder, D.M. (2018). Effect of torpor on host transcriptomic
538 responses to a fungal pathogen in hibernating bats. Mol. Ecol.

539 Frank, C.L., Michalski, A., McDonough, A.A., Rahimian, M., Rudd, R.J., and Herzog, C.
540 (2014). The resistance of a North American bat species (Eptesicus fuscus) to White-Nose
541 Syndrome (WNS). PLoS ONE *9*, e113958.

542 Frick, W.F., Pollock, J.F., Hicks, A.C., Langwig, K.E., Reynolds, D.S., Turner, G.G.,
543 Butchkoski, C.M., and Kunz, T.H. (2010). An Emerging disease causes regional population
544 collapse of a common North American bat species. Science *329*, 679–682.

545 Frick, W.F., Puechmaille, S.J., Hoyt, J.R., Nickel, B.A., Langwig, K.E., Foster, J.T., Barlow,
546 K.E., Bartonička, T., Feller, D., Haarsma, A.-J., et al. (2015). Disease alters macroecological
547 patterns of North American bats. Glob. Ecol. Biogeogr. *24*, 741–749.

548 Frick, W.F., Cheng, T.L., Langwig, K.E., Hoyt, J.R., Janicki, A.F., Parise, K.L., Foster, J.T.,
549 and Kilpatrick, A.M. (2017). Pathogen dynamics during invasion and establishment of white-
550 nose syndrome explain mechanisms of host persistence. Ecology *98*, 624–631.

551 Gallana, M., Ryser-Degiorgis, M.-P., Wahli, T., and Segner, H. (2013). Climate change and
552 infectious diseases of wildlife: Altered interactions between pathogens, vectors and hosts. Curr.
553 Zool. *59*, 427–437.

554 Gignoux-Wolfsohn, S.A., Pinsky, M.L., Kerwin, K., Herzog, C., Hall, M., Bennett, A.B.,
555 Fefferman, N.H., and Maslo, B. (2018). Genomic signatures of evolutionary rescue in bats
556 surviving white-nose syndrome. BioRxiv 470294.

557 Grieneisen, L.E., Brownlee-Bouboulis, S.A., Johnson, J.S., and Reeder, D.M. (2015). Sex and
558 hibernaculum temperature predict survivorship in white-nose syndrome affected little brown
559 myotis (Myotis lucifugus). R. Soc. Open Sci. *2*, 140470.

560 Groot, N.G. de, Otting, N., Doxiadis, G.G.M., Balla-Jhagjhoorsingh, S.S., Heeney, J.L., Rood,
561 J.J. van, Gagneux, P., and Bontrop, R.E. (2002). Evidence for an ancient selective sweep in the
562 MHC class I gene repertoire of chimpanzees. Proc. Natl. Acad. Sci. *99*, 11748–11753.

563 Hansen, M.M., Olivieri, I., Waller, D.M., and Nielsen, E.E. (2012). Monitoring adaptive
564 genetic responses to environmental change. Mol. Ecol. *21*, 1311–1329.

565 Harazim, M., Horáček, I., Jakešová, L., Luermann, K., Moravec, J.C., Morgan, S., Pikula, J.,
566 Sosík, P., Vavrušová, Z., Zahradníková, A., et al. (2018). Natural selection in bats with
567 historical exposure to white-nose syndrome. BMC Zool. *3*, 8.

568 Hayman, D.T.S., Pulliam, J.R.C., Marshall, J.C., Cryan, P.M., and Webb, C.T. (2016).
569 Environment, host, and fungal traits predict continental-scale white-nose syndrome in bats. Sci.
570 Adv. *2*, e1500831.

571 Hoekstra, H.E., Hirschmann, R.J., Bundey, R.A., Insel, P.A., and Crossland, J.P. (2006). A
572 single amino acid mutation contributes to adaptive beach mouse color pattern. Science *313*,
573 101–104.

574 Huang, X., Huang, T., Deng, W., Yan, G., Qiu, H., Huang, Y., Ke, S., Hou, Y., Zhang, Y.,
575 Zhang, Z., et al. (2017). Genome-wide association studies identify susceptibility loci affecting
576 respiratory disease in Chinese Erhualian pigs under natural conditions. Anim. Genet. *48*, 30–
577 37.

578 Huang, Z., Ruan, H.-B., Xian, L., Chen, W., Jiang, S., Song, A., Wang, Q., Shi, P., Gu, X., and
579 Gao, X. (2014). The stem cell factor/Kit signalling pathway regulates mitochondrial function
580 and energy expenditure. Nat. Commun. *5*, 4282.

581 Humphries, M.M., Thomas, D.W., and Speakman, J.R. (2002). Climate-mediated energetic
582 constraints on the distribution of hibernating mammals. Nature *418*, 313–316.

583 Jeffery, K.J., and Bangham, C.R. (2000). Do infectious diseases drive MHC diversity?
584 Microbes Infect. *2*, 1335–1341.

585 Johnson, J.S., Reeder, D.M., McMichael, J.W., Meierhofer, M.B., Stern, D.W.F., Lumadue,
586 S.S., Sigler, L.E., Winters, H.D., Vodzak, M.E., Kurta, A., et al. (2014). Host, pathogen, and
587 environmental characteristics predict white-nose syndrome mortality in captive little brown
588 myotis (*Myotis lucifugus*). Plos One *9*, e112502.

589 Karlsson, E.K., Kwiatkowski, D.P., and Sabeti, P.C. (2014). Natural selection and infectious
590 disease in human populations. Nat. Rev. Genet. *15*, 379–393.

591 Kilpatrick, A.M. (2006). Facilitating the evolution of resistance to avian malaria in Hawaiian
592 birds. Biol. Conserv. *128*, 475–485.

593 Kofler, R., Pandey, R.V., and Schlötterer, C. (2011). PoPoolation2: identifying differentiation
594 between populations using sequencing of pooled DNA samples (Pool-Seq). Bioinformatics *27*,
595 3435–3436.

596 Kyle, C.J., Rico, Y., Castillo, S., Srithayakumar, V., Cullingham, C.I., White, B.N., and Pond,
597 B.A. (2014). Spatial patterns of neutral and functional genetic variations reveal patterns of local
598 adaptation in raccoon (Procyon lotor) populations exposed to raccoon rabies. Mol. Ecol. *23*,
599 2287–2298.

600 Langmead, B., and Salzberg, S.L. (2012). Fast gapped-read alignment with Bowtie 2. Nat.
601 Methods *9*, 357–359.

602 Langwig, K.E., Frick, W.F., Reynolds, R., Parise, K.L., Drees, K.P., Hoyt, J.R., Cheng, T.L.,
603 Kunz, T.H., Foster, J.T., and Kilpatrick, A.M. (2015). Host and pathogen ecology drive the
604 seasonal dynamics of a fungal disease, white-nose syndrome. Proc. R. Soc. B-Biol. Sci. *282*,
605 20142335.

606 Langwig, K.E., Hoyt, J.R., Parise, K.L., Frick, W.F., Foster, J.T., and Kilpatrick, A.M. (2017).
607 Resistance in persisting bat populations after white-nose syndrome invasion. Phil Trans R Soc
608 B *372*, 20160044.

609 Lemieux-Labonté, V., Simard, A., Willis, C.K.R., and Lapointe, F.-J. (2017). Enrichment of
610 beneficial bacteria in the skin microbiota of bats persisting with white-nose syndrome.
611 Microbiome *5*, 115.

612 Li, H., Handsaker, B., Wysoker, A., Fennell, T., Ruan, J., Homer, N., Marth, G., Abecasis, G.,
613 Durbin, R., and 1000 Genome Project Data Processing Subgroup (2009). The Sequence
614 Alignment/Map format and SAMtools. Bioinforma. Oxf. Engl. *25*, 2078–2079.

615 Lilley, T., Anttila, J., and Ruokolainen, L. (2018). Landscape structure and ecology influence
616 the spread of a bat fungal disease. Funct. Ecol. *0*.

617 Lilley, T.M., Johnson, J.S., Ruokolainen, L., Rogers, E.J., Wilson, C., Schell, S.M., Field,
618 K.A., and Reeder, D.M. (2016). White-nose syndrome survivors do not exhibit frequent
619 arousals associated with *Pseudogymnoascus destructans* infection. Front. Zool. *13*, 12.

620 Lilley, T.M., Prokkola, J.M., Johnson, J.S., Rogers, E.J., Gronsky, S., Kurta, A., Reeder, D.M.,
621 and Field, K.A. (2017). Immune responses in hibernating little brown myotis (*Myotis lucifugus*)
622 with white-nose syndrome. Proc R Soc B *284*, 20162232.

623 Lilley, T.M., Prokkola, J.M., Blomberg, A.S., Paterson, S., Johnson, J.S., Turner, G.G.,
624 Bartonička, T., Bachorec, E., Reeder, D.M., and Field, K.A. (2019). Resistance is futile: RNA-
625 sequencing reveals differing responses to bat fungal pathogen in Nearctic Myotis lucifugus and
626 Palearctic Myotis myotis. Oecologia.

627 Lips, K.R., Brem, F., Brenes, R., Reeve, J.D., Alford, R.A., Voyles, J., Carey, C., Livo, L.,
628 Pessier, A.P., and Collins, J.P. (2006). Emerging infectious disease and the loss of biodiversity
629 in a Neotropical amphibian community. Proc. Natl. Acad. Sci. U. S. A. *103*, 3165–3170.

630 Lorch, J.M., Meteyer, C.U., Behr, M.J., Boyles, J.G., Cryan, P.M., Hicks, A.C., Ballmann,
631 A.E., Coleman, J.T.H., Redell, D.N., Reeder, D.M., et al. (2011). Experimental infection of
632 bats with *Geomyces destructans* causes white-nose syndrome. Nature *480*, 376-U129.

633 Lorch, J.M., Muller, L.K., Russell, R.E., O'Connor, M., Lindner, D.L., and Blehert, D.S.
634 (2013). Distribution and environmental persistence of the causative agent of white-nose
635 syndrome, *Geomyces destructans*, in bat hibernacula of the Eastern United States. Appl.
636 Environ. Microbiol. *79*, 1293–1301.

637 Luikart, G., Allendorf, F.W., Cornuet, J.-M., and Sherwin, W.B. (1998). Distortion of allele
638 frequency distributions provides a test for recent population bottlenecks. J. Hered. *89*, 238–
639 247.

640 Luis, A.D., and Hudson, P.J. (2006). Hibernation patterns in mammals: a role for bacterial
641 growth? Funct. Ecol. *20*, 471–477.

642 Marroquin, C.M., Lavine, J.O., and Windstam, S.T. (2017). Effect of Humidity on
643 Development of Pseudogymnoascus destructans, the Causal Agent of Bat White-Nose
644 Syndrome. Northeast. Nat. *24*, 54–64.

645 Maslo, B., and Fefferman, N.H. (2015). A case study of bats and white-nose syndrome
646 demonstrating how to model population viability with evolutionary effects. Conserv. Biol. *29*,
647 1176–1185.

648 Maslo, B., Valent, M., Gumbs, J.F., and Frick, W.F. (2015). Conservation implications of
649 ameliorating survival of little brown bats with white-nose syndrome. Ecol. Appl. *25*, 1832–
650 1840.

651 McGuire, L.P., Mayberry, H.W., and Willis, C.K.R. (2017). White-nose syndrome increases
652 torpid metabolic rate and evaporative water loss in hibernating bats. Am. J. Physiol.-Regul.
653 Integr. Comp. Physiol. *313*, R680–R686.

654 McKenna, A., Hanna, M., Banks, E., Sivachenko, A., Cibulskis, K., Kernytsky, A., Garimella,
655 K., Altshuler, D., Gabriel, S., Daly, M., et al. (2010). The Genome Analysis Toolkit: a
656 MapReduce framework for analyzing next-generation DNA sequencing data. Genome Res. *20*,
657 1297–1303.

658 Messer, P.W., and Petrov, D.A. (2013). Population genomics of rapid adaptation by soft
659 selective sweeps. Trends Ecol. Evol. *28*, 659–669.

660 Meteyer, C.U., Barber, D., and Mandl, J.N. (2012). Pathology in euthermic bats with white
661 nose syndrome suggests a natural manifestation of immune reconstitution inflammatory
662 syndrome. Virulence *3*, 583–588.

663 Micalizzi, E.W., Mack, J.N., White, G.P., Avis, T.J., and Smith, M.L. (2017). Microbial
664 inhibitors of the fungus *Pseudogymnoascus destructans*, the causal agent of white-nose
665 syndrome in bats. PLOS ONE *12*, e0179770.

666 Miller, C.T., Beleza, S., Pollen, A.A., Schluter, D., Kittles, R.A., Shriver, M.D., and Kingsley,
667 D.M. (2007). Cis-regulatory changes in Kit ligand expression and parallel evolution of
668 pigmentation in sticklebacks and humans. Cell *131*, 1179–1189.

669 Miller-Butterworth, C.M., Vonhof, M.J., Rosenstern, J., Turner, G.G., and Russell, A.L.
670 (2014). Genetic structure of little brown bats (Myotis lucifugus) corresponds with spread of
671 white-nose syndrome among hibernacula. J. Hered. esu012.

672 Minnis, A.M., and Lindner, D.L. (2013). Phylogenetic evaluation of Geomyces and allies
673 reveals no close relatives of Pseudogymnoascus destructans, comb. nov., in bat hibernacula of
674 eastern North America. Fungal Biol. *117*, 638–649.

675 Morales, A.E., and Carstens, B.C. (2018). Evidence that Myotis lucifugus "Subspecies" are
676 Five Nonsister Species, Despite Gene Flow. Syst. Biol. *67*, 756–769.

677 Norquay, K.J.O., Martinez-Nuñez, F., Dubois, J.E., Monson, K.M., and Willis, C.K.R. (2013).
678 Long-distance movements of little brown bats (Myotis lucifugus). J. Mammal. *94*, 506–515.

679 Paterson, S., Wilson, K., and Pemberton, J.M. (1998). Major histocompatibility complex
680 variation associated with juvenile survival and parasite resistance in a large unmanaged
681 ungulate population (Ovis aries L.). Proc. Natl. Acad. Sci. *95*, 3714–3719.

682 Paterson, S., Vogwill, T., Buckling, A., Benmayor, R., Spiers, A.J., Thomson, N.R., Quail, M.,
683 Smith, F., Walker, D., Libberton, B., et al. (2010). Antagonistic coevolution accelerates
684 molecular evolution. Nature *464*, 275–278.

685 Peters, J.-M., Tedeschi, A., and Schmitz, J. (2008). The cohesin complex and its roles in
686 chromosome biology. Genes Dev. *22*, 3089–3114.

687 Puechmaille, S.J., Wibbelt, G., Korn, V., Fuller, H., Forget, F., Mühldorfer, K., Kurth, A.,
688 Bogdanowicz, W., Borel, C., Bosch, T., et al. (2011). Pan-European distribution of white-nose
689 syndrome fungus (*Geomyces destructans*) not associated with mass mortality. PLoS ONE *6*,
690 e19167.

691 R Development Core Team (2011). R: A language and environment for statistical computing.

692 Råberg, L., Graham, A.L., and Read, A.F. (2009). Decomposing health: tolerance and
693 resistance to parasites in animals. Philos. Trans. R. Soc. Lond. B. Biol. Sci. *364*, 37–49.

694 Reeder, D.M., Frank, C.L., Turner, G.G., Meteyer, C.U., Kurta, A., Britzke, E.R., Vodzak,
695 M.E., Darling, S.R., Stihler, C.W., Hicks, A.C., et al. (2012). Frequent arousal from hibernation
696 linked to severity of infection and mortality in bats with white-nose syndrome. Plos One *7*,
697 e38920.

698 Ren, P., Haman, K.H., Last, L.A., Rajkumar, S.S., Keel, M.K., and Chaturvedi, V. (2012).
699 Clonal Spread of Geomyces destructans among Bats, Midwestern and Southern United States.
700 Emerg. Infect. Dis. *18*, 883–885.

701 Rico, Y., Morris-Pocock, J., Zigouris, J., Nocera, J.J., and Kyle, C.J. (2015). Lack of Spatial
702 Immunogenetic Structure among Wolverine (Gulo gulo) Populations Suggestive of Broad
703 Scale Balancing Selection. PLOS ONE *10*, e0140170.

704 van Riper, C., van Riper, S.G., Goff, M.L., and Laird, M. (1986). The Epizootiology and
705 Ecological Significance of Malaria in Hawaiian Land Birds. Ecol. Monogr. *56*, 327–344.

706 Robinson, S.J., Samuel, M.D., Johnson, C.J., Adams, M., and McKenzie, D.I. (2012).
707 Emerging prion disease drives host selection in a wildlife population. Ecol. Appl. Publ. Ecol.
708 Soc. Am. *22*, 1050–1059.

709 Routtu, J., and Ebert, D. (2015). Genetic architecture of resistance in *Daphnia* hosts against
710 two species of host-specific parasites. Heredity *114*, 241–248.

711 Scholthof, K.-B.G. (2007). The disease triangle: pathogens, the environment and society. Nat.
712 Rev. Microbiol. *5*, 152–156.

713 Schoville, S.D., Bonin, A., François, O., Lobreaux, S., Melodelima, C., and Manel, S. (2012).
714 Adaptive Genetic Variation on the Landscape: Methods and Cases. Annu. Rev. Ecol. Evol.
715 Syst. *43*, 23–43.

716 Sironi, M., Cagliani, R., Forni, D., and Clerici, M. (2015). Evolutionary insights into host–
717 pathogen interactions from mammalian sequence data. Nat. Rev. Genet. *16*, 224–236.

718 Smith, K.F., Sax, D.F., and Lafferty, K.D. (2006). Evidence for the Role of Infectious Disease
719 in Species Extinction and Endangerment. Conserv. Biol. *20*, 1349–1357.

720 Sparks, A.M., Watt, K., Sinclair, R., Pilkington, J.G., Pemberton, J.M., McNeilly, T.N.,
721 Nussey, D.H., and Johnston, S.E. (2019). The genetic architecture of helminth-specific immune
722 responses in a wild population of Soay sheep (Ovis aries). BioRxiv 628271.

723 Spurgin, L.G., and Richardson, D.S. (2010). How pathogens drive genetic diversity: MHC,
724 mechanisms and misunderstandings. Proc. Biol. Sci. *277*, 979–988.

725 Studier, E.H., and O'Farrell, M.J. (1972). Biology of Myotis thysanodes and M. lucifugus
726 (Chiroptera: Vespertilionidae). I. Thermoregulation. Comp. Biochem. Physiol. A *41*, 567–595.

727 Teacher Amber G. F., Garner Trenton W. J., and Nichols Richard A. (2009). Population genetic
728 patterns suggest a behavioural change in wild common frogs (Rana temporaria) following
729 disease outbreaks (Ranavirus). Mol. Ecol. *18*, 3163–3172.

730 The UniProt Consortium (2019). UniProt: a worldwide hub of protein knowledge. Nucleic
731 Acids Res. *47*, D506–D515.

732 Thomas, D.W., Dorais, M., and Bergeron, J.-M. (1990). Winter Energy Budgets and Cost of
733 Arousals for Hibernating Little Brown Bats, Myotis lucifugus. J. Mammal. *71*, 475–479.

734 Tompkins, D.M., Carver, S., Jones, M.E., Krkošek, M., and Skerratt, L.F. (2015). Emerging
735 infectious diseases of wildlife: a critical perspective. Trends Parasitol. *31*, 149–159.

736 Turner, G.G., Reeder, D.M., and Coleman, J.T.H. (2011). A five-year assessment of mortality
737 and geographic spread of white-nose syndrome in North American bats and a look to the future.
738 Bat Res. News *52*, 13–27.

739 Verant, M.L., Boyles, J.G., Waldrep, W., Wibbelt, G., and Blehert, D.S. (2012). Temperature-
740 dependent growth of *Geomyces destructans*, the fungus that causes bat white-nose syndrome.
741 Plos One *7*, e46280.

742 Verant, M.L., Meteyer, C.U., Speakman, J.R., Cryan, P.M., Lorch, J.M., and Blehert, D.S.
743 (2014). White-nose syndrome initiates a cascade of physiologic disturbances in the hibernating
744 bat host. BMC Physiol. *14*, 10.

745 Vonhof, M.J., Russell, A.L., and Miller-Butterworth, C.M. (2015). Range-wide genetic
746 analysis of little brown bat (Myotis lucifugus) populations: estimating the risk of spread of
747 White-nose syndrome. PLoS ONE *10*, e0128713.

748 Vonhof, M.J., Amelon, S.K., Currie, R.R., and McCracken, G.F. (2016). Genetic structure of
749 winter populations of the endangered Indiana bat (Myotis sodalis) prior to the white nose

750 syndrome epidemic: implications for the risk of disease spread. Conserv. Genet. *17*, 1025–
751 1040.

752 Voronin, D.A., and Kiseleva, E.V. (2007). [Functional role of proteins containing ankyrin
753 repeats]. Tsitologiia *49*, 989–999.

754 Warnecke, L., Turner, J.M., and Geiser, F. (2008). Torpor and basking in a small arid zone
755 marsupial. Naturwissenschaften *95*, 73–78.

756 Warnecke, L., Turner, J.M., Bollinger, T.K., Lorch, J.M., Misra, V., Cryan, P.M., Wibbelt, G.,
757 Blehert, D.S., and Willis, C.K.R. (2012). Inoculation of bats with European *Geomyces*
758 *destructans* supports the novel pathogen hypothesis for the origin of white-nose syndrome.
759 Proc. Natl. Acad. Sci. U. S. A. *109*, 6999–7003.

760 Warnecke, L., Turner, J.M., Bollinger, T.K., Misra, V., Cryan, P.M., Blehert, D.S., Wibbelt,
761 G., and Willis, C.K.R. (2013). Pathophysiology of white-nose syndrome in bats: a mechanistic
762 model linking wing damage to mortality. Biol. Lett. *9*, 20130177.

763 Wibbelt, G., Kurth, A., Hellmann, D., Weishaar, M., Barlow, A., Veith, M., Prueger, J.,
764 Goerfoel, T., Grosche, L., Bontadina, F., et al. (2010). White-nose syndrome fungus
765 (*Geomyces destructans*) in Bats, Europe. Emerg. Infect. Dis. *16*, 1237–1243.

766 Wibbelt, G., Puechmaille, S.J., Ohlendorf, B., Muehldorfer, K., Bosch, T., Goerfoel, T.,
767 Passior, K., Kurth, A., Lacremans, D., and Forget, F. (2013). Skin lesions in European
768 hibernating bats associated with *Geomyces destructans*, the etiologic agent of white-nose
769 syndrome. Plos One *8*, e74105.

770 Wilder, A.P., Kunz, T.H., and Sorenson, M.D. (2015). Population genetic structure of a
771 common host predicts the spread of white-nose syndrome, an emerging infectious disease in
772 bats. Mol. Ecol. *24*, 5495–5506.

773 Willis, C.K.R., Menzies, A.K., Boyles, J.G., and Wojciechowski, M.S. (2011). Evaporative
774 water loss is a plausible explanation for mortality of bats from white-nose syndrome. Integr.
775 Comp. Biol. *51*, 364–373.

776 Wright, S. (1978). Evolution and the Genetics of Populations, Volume 4. Variability within
777 and among Natural Populations. (Chicago: University of Chicago Press).

778 www.whitenosesyndrome.org (2019). White-nose syndrome occurance map - by year (2019).
779 Data last updated: 3/15/2019. Available at:
780 https://www.whitenosesyndrome.org/resources/map.

781 Yang, Z., Shi, H., Ma, P., Zhao, S., Kong, Q., Bian, T., Gong, C., Zhao, Q., Liu, Y., Qi, X., et
782 al. (2018). Darwinian Positive Selection on the Pleiotropic Effects of KITLG Explain Skin
783 Pigmentation and Winter Temperature Adaptation in Eurasians. Mol. Biol. Evol. 1–12.

784 Zeisset, I., and Beebee, T.J.C. (2014). Drift Rather than Selection Dominates MHC Class II
785 Allelic Diversity Patterns at the Biogeographical Range Scale in Natterjack Toads Bufo
786 calamita. PLOS ONE *9*, e100176.

787 Zhang, T., Victor, T.R., Rajkumar, S.S., Li, X., Okoniewski, J.C., Hicks, A.C., Davis, A.D.,
788 Broussard, K., LaDeau, S.L., Chaturvedi, S., et al. (2014). Mycobiome of the bat white nose
789 syndrome affected caves and mines reveals diversity of fungi and local adaptation by the fungal
790 pathogen *Pseudogymnoascus (Geomyces) destructans*. PLOS ONE *9*, e108714.

791 Zhang, T., Chaturvedi, V., and Chaturvedi, S. (2015). Novel *Trichoderma polysporum* strain
792 for the biocontrol of *Pseudogymnoascus destructans*, the fungal etiologic agent of bat white
793 nose syndrome. PLOS ONE *10*, e0141316.

794 Zukal, J., Bandouchova, H., Brichta, J., Cmokova, A., Jaron, K.S., Kolarik, M., Kovacova, V.,
795 Kubátová, A., Nováková, A., Orlov, O., et al. (2016). White-nose syndrome without borders:
796 *Pseudogymnoascus destructans* infection tolerated in Europe and Palearctic Asia but not in
797 North America. Sci. Rep. *6*, 19829.

798 **Table captions**

799 Table 1. Samples used in study.

800 Table 2. Summary of individual SNP F_{ST} values across the *M. lucifugus* genome when
801 comparing Pre-WNS with Post-WNS; and samples from PA and NY (both Pre- and Post-
802 WNS).

803 Table 3. Genes within the *M. lucifugus* genome – excluding scaffold GL429776 – with
804 windows possessing F_{ST} values >= 0.05 when comparing PA and NY samples Post-WNS

805 Table 4. Genes within scaffold GL429776 with windows possessing F_{ST} values >= 0.05 when
806 comparing PA and NY samples Post-WNS.

807 Figure captions

808 Fig. 1. *M. lucifugus* sampling locations in Pennsylvania (PA) and New York (NY). Pre-WNS-
809 sites in grey circles and Post-WNS-sites in white circles. 1) Aitkin Cave, Mifflin County, PA;
810 2) Snyder County, Penn, PA; 3) Lewisburg, Union Co, PA; 4) Northumberland County, PA;

811 5) Howes Cave, County Schoharie, NY; 6) Allentown, Lehigh County, PA; 7) Woodward,
812 Centre County, PA; 8) Alexandria, Huntingdon County, PA; 9) Lackawaxen, Pike County, PA;
813 10) Oley, County Berks, PA; 11) Frankstown, County Blair, PA; 12) Williams Preserve Mine,
814 NY; 13) Hoopers Mine, NY; 14) Delmar, Albany County, NY; and 15) Willsboro, Essex
815 County, NY.

816 Fig. 2. Fixation indices (F_{ST}) across the *M. lucifugus* genome, comparing the population before
817 and after the arrival of white-nose syndrome. Scaffold lengths presented in green and blue.
818 Solid red line indicates cut-off for F_{ST} values of 5 standard deviations from the mean across
819 the whole genome; dotted red line indicates cut-off of F_{ST}=0.05.

820 Fig 3. Fixation indices (F_{ST}) across the *M. lucifugus* genome between geographically separated
821 individuals of the study population a) comparing individuals from PA to individuals from NY
822 before the arrival of WNS; b) comparing individuals from PA before and after the arrival of
823 WNS; and c) comparing individuals from NY before and after the arrival of WNS. Solid red
824 line indicates cut-off for F_{ST} values of 5 standard deviations from the mean across the whole
825 genome; dotted red line indicates cut-off of F_{ST}=0.05.

826 Fig 4. Fixation indices (F_{ST}) across the *M. lucifugus* genome between geographically separated
827 individuals of the study population a) comparing individuals from PA to individuals from NY
828 after the arrival of WNS, with a zoomed plot of scaffold GL429776 and gene models therein
829 containing windows demonstrating F_{ST} values < 0.05; and b) comparing individuals from PA
830 to individuals from NY with Pre- and Post-WNS data combined. Solid red line indicates cut-
831 off for F_{ST} values of 5 standard deviations from the mean across the whole genome; dotted red
832 line indicates cut-off of F_{ST}=0.05.

833 Fig 5. Proportions of reference alleles called at individual SNP sites for the region of scaffold
834 GL429776 demonstrating high F_{ST} values when comparing a) individuals from Pennsylvania
835 before and after the arrival of WNS; b) individuals from NY before and after the arrival of
836 WNS; c) individuals from PA to individuals from NY before the arrival of WNS; and d)
837 individuals from PA to individuals from NY after the arrival of WNS.

838 Table 1.

Sample age	Classification	Total number of samples	Pennsylvania*	New York*
2006	Pre-WNS	49	25	24
2007	Pre-WNS	3	3	
2015	Post-WNS	28	28	
2016	Post-WNS	139	82	57

* WNS first detected in New York in 2007 and PA in 2009

839

Table 2.

	Pre- vs post-WNS	**Between site (combining pre- and post-WNS)**
Median (Interquartile range)	0.0059 (0.0013 – 0.0171)	0.0057 (0.0013 – 0.0165)
Mean (s.d.)	0.0127 (0.0173)	0.0123 (0.0170)

Table 3.

Scaffold	Location range (bp)	Gene ID	Protein Function	Number of overlapping high F_{ST} windows
NW_005871715.1	288334 - 351644	102435296	bifunctional heparan sulfate N-deacetylase/N-sulfotransferase 4-like (partial)	4
NW_005871771.1	26662 - 48938	102441697	E3 ubiquitin-protein ligase TRIM7	1
NW_005871823.1	81353 - 213965	102428352	Ankyrin 2	7
NW_005871905.1	175 - 139344	102428043	calcium/calmodulin-dependent protein kinase type II subunit delta-like	10

NW_005872026.1	72042 - 101269	102443179	N-deacetylase and N-sulfotransferase 4 (partial)	1
NW_005872062.1	33266 - 86607	102428048	zinc finger GRF-type containing 1	1

Table 4.

Gene ID	F_{ST}	No of windows	No of windows	Start pos.	End pos.	Details

			(per 10kb)			
MGAT4C	0.0612	78	1.08	8999210	9724150	Glycosyltransferase that participates in the transfer of N-acetylglucosamine (GlcNAc) to the core mannose residues of N-linked glycans
CEP290	0.0679	12	1.01	10709418	10827912	Involved in early and late steps in cilia formation
ATP2B1	0.0826	12	0.89	12228178	12362389	The protein encoded by this gene belongs to the family of P-type primary ion transport ATPases characterised by the formation of an aspartyl phosphate intermediate during the reaction cycle. These enzymes remove bivalent calcium ions from eukaryotic cells against very large concentration gradients and play a critical role in intracellular calcium homeostasis.

KITLG	0.0706	10	1.13	11127130	11215731	Plays an essential role in the regulation of cell survival and proliferation, hematopoiesis, stem cell maintenance, gametogenesis, mast cell development, migration and function, and in melanogenesis.
POC1B	0.0686	7	0.74	12044678	12139811	Plays an important role in centriole assembly and/or stability and ciliogenesis
TMTC3	0.0872	6	1.00	10827719	10887502	Involved in the positive regulation of proteasomal protein degradation in the endoplasmic reticulum (ER), and the control of ER stress response.
GeneID:111824954	0.0693	5	1.14	11756928	11800690	uncharacterised LOC111824954
CUNH12orf50	0.0588	2	0.67	10663328	10693373	chromosome unknown C12orf50 homolog
GeneID:111824948	0.0816	2	1.13	11375011	11392720	uncharacterised LOC111824948

GeneID:111824949	0.0635	2	1.14	11802704	11820273	uncharacterised LOC111824949
CUNH12orf29	0.0488	1	0.71	10696290	10710421	chromosome unknown C12orf29 homolog
DUSP6	0.0603	1	2.26	11976039	11980455	Inactivates MAP kinases.
GeneID:111824955	0.0459	1	1.57	12101754	12108133	uncharacterised LOC111824955

Fig 1.

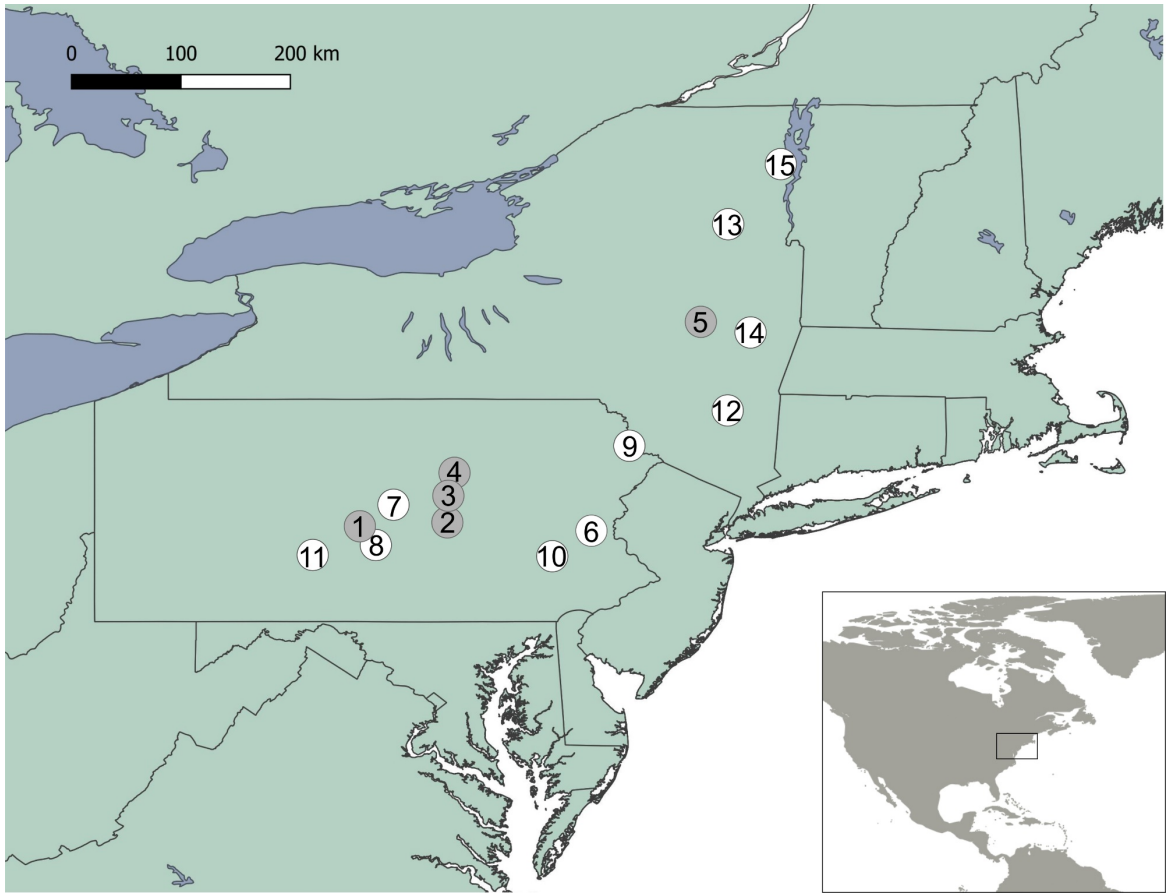

Fig. 2.

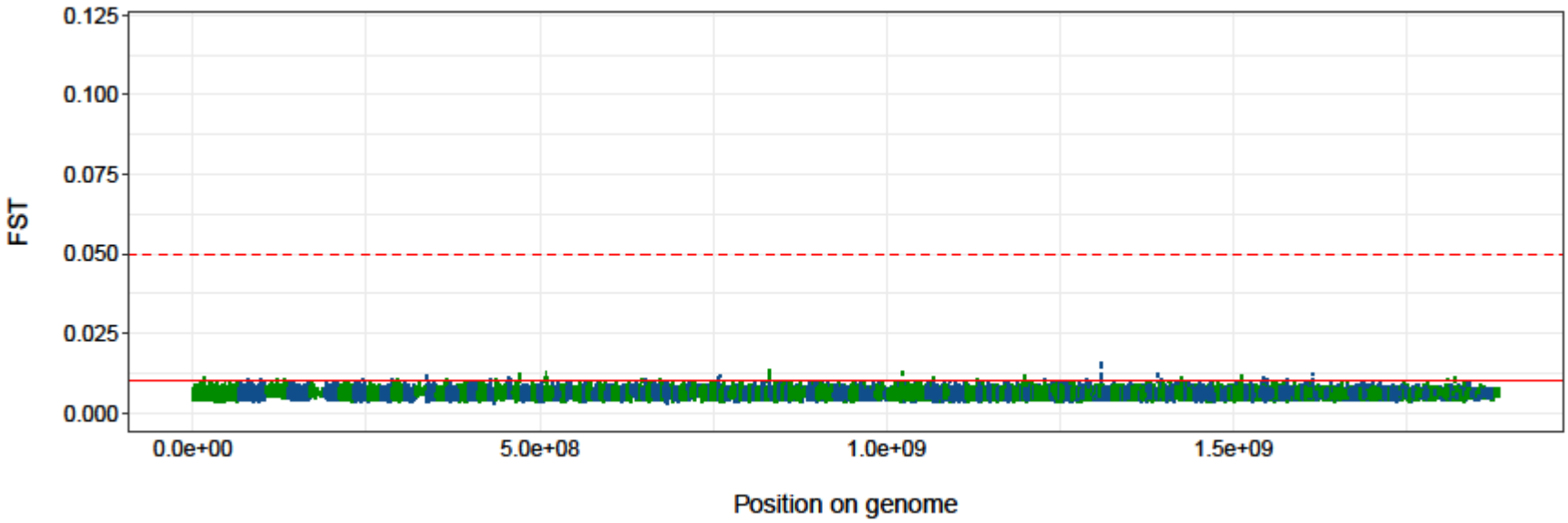
0.125
0.100
0.075
0.050
0.025
0.000
FST
0.0e+00
5.0e+08
1.0e+09
1.5e+09
Position on genome

Fig. 3.

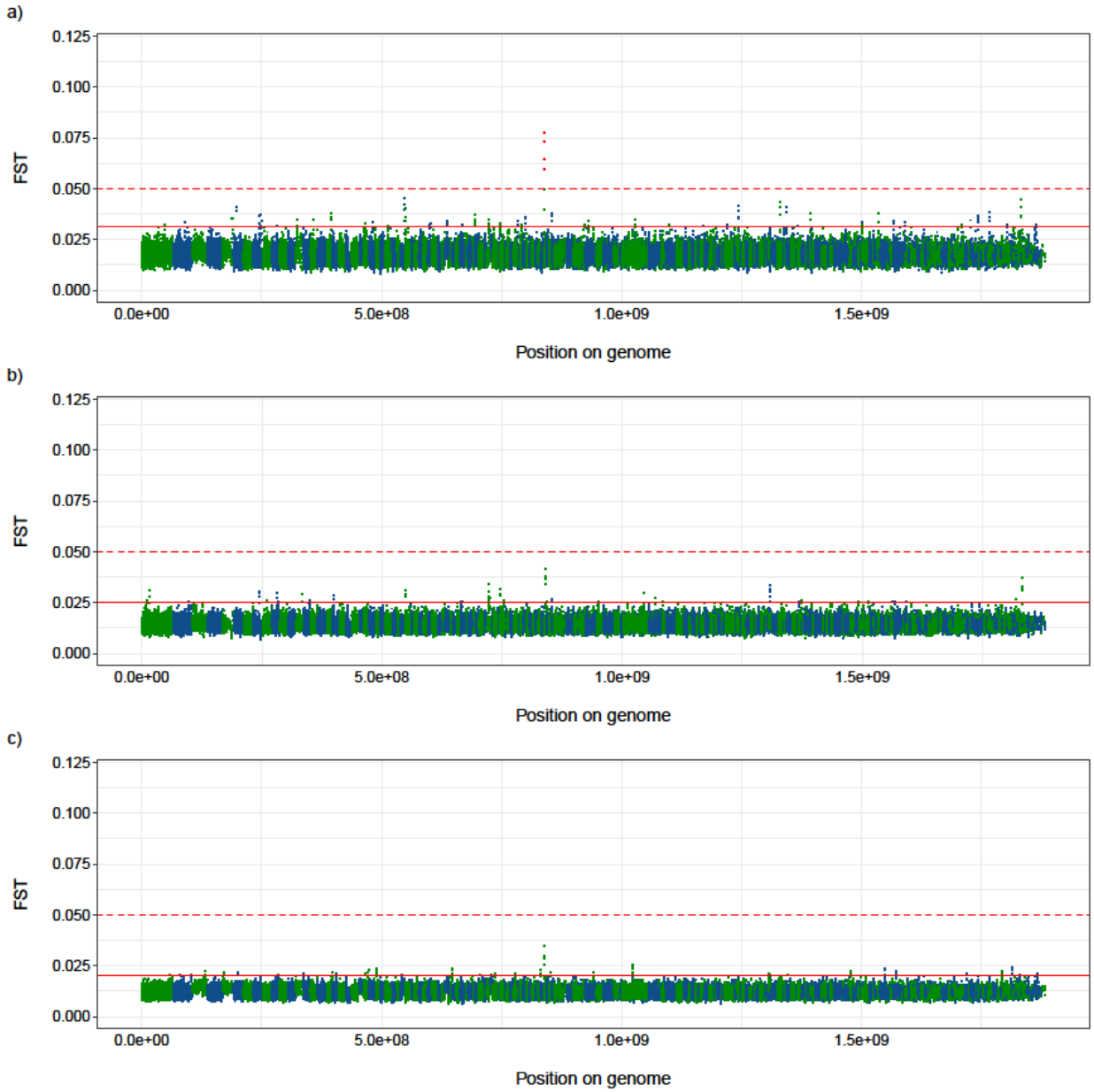
a)
FST
0.125
0.100
0.075
0.050
0.025
0.000
0.0e+00
5.0e+08
1.0e+09
1.5e+09
Position on genome
b)
FST
0.125
0.100
0.075
0.050
0.025
0.000
0.0e+00
5.0e+08
1.0e+09
1.5e+09
Position on genome
c)
FST
0.125
0.100
0.075
0.050
0.025
0.000
0.0e+00
5.0e+08
1.0e+09
1.5e+09
Position on genome

Fig 4.

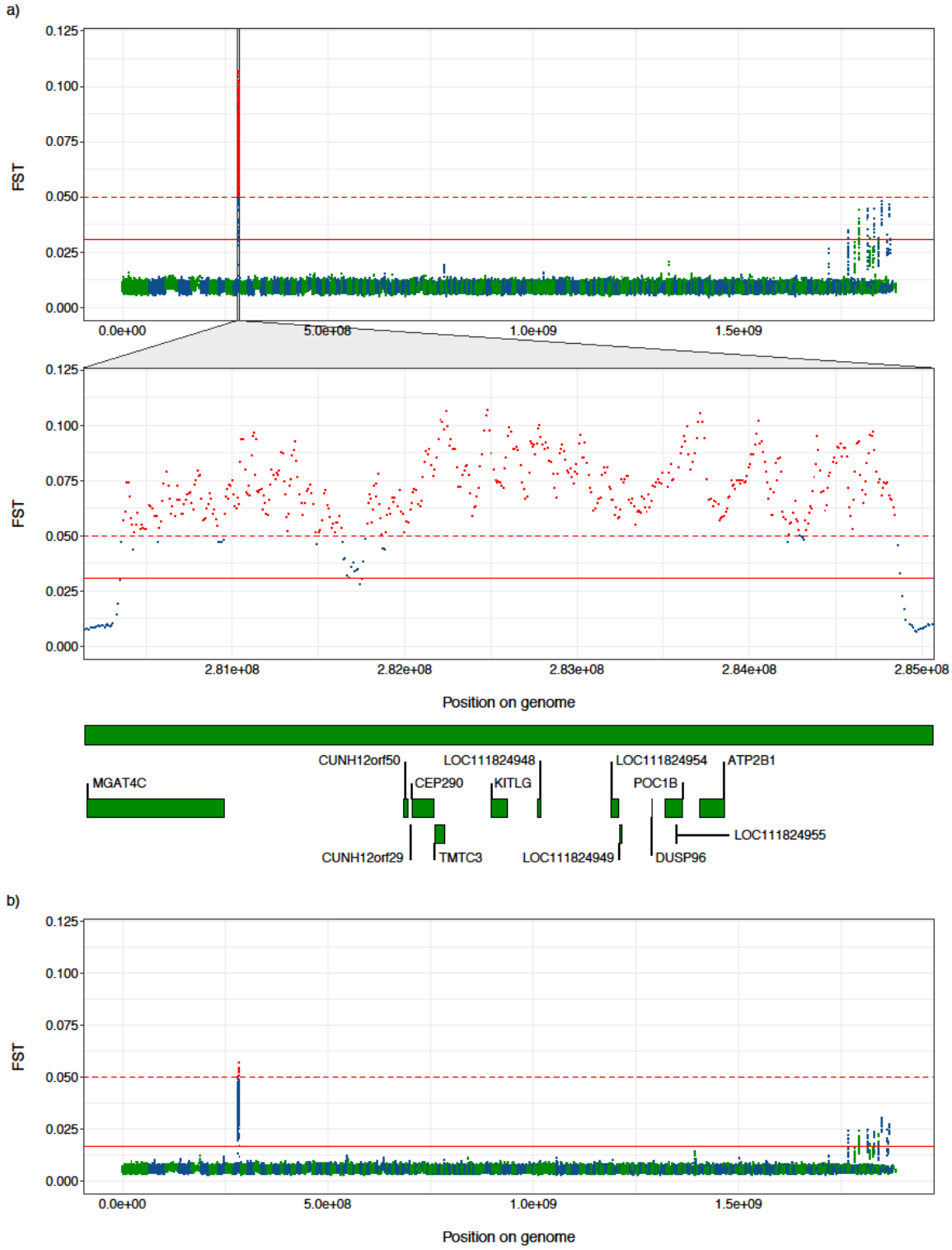
a)
FST
0.125
0.100
0.075
0.050
0.025
0.000
0.0e+00
5.0e+08
1.0e+09
1.5e+09
2.81e+08
2.82e+08
2.83e+08
2.84e+08
2.85e+08
Position on genome
MGAT4C
CUNH12orf50
CEP290
LOC111824948
KITLG
LOC111824954
POC1B
ATP2B1
LOC111824955
CUNH12orf29
TMTC3
LOC111824949
DUSP96
b)
FST
0.125
0.100
0.075
0.050
0.025
0.000
0.0e+00
5.0e+08
1.0e+09
1.5e+09
Position on genome

Fig 5.

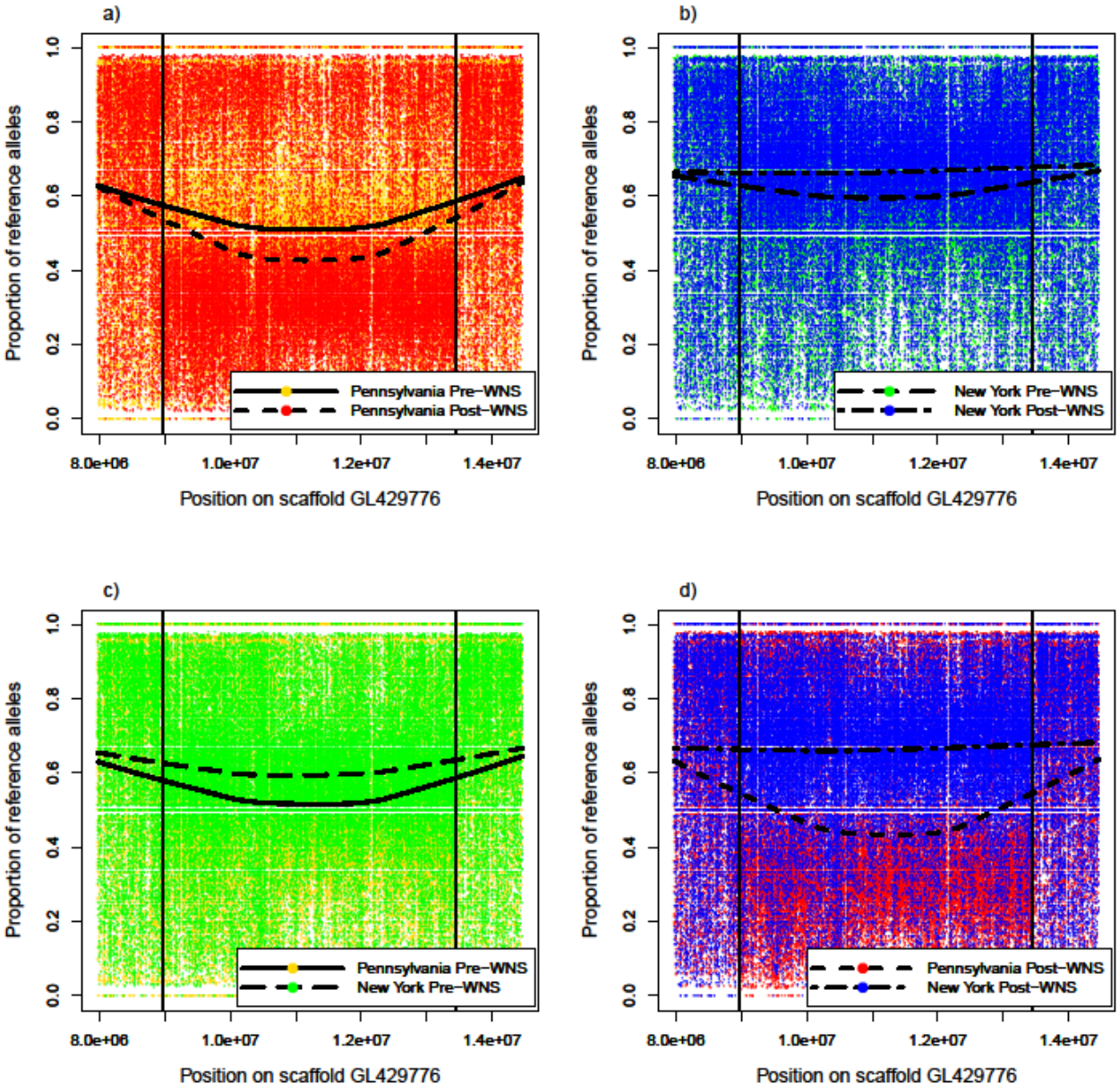
a)
b)
c)
d)
Proportion of reference alleles
0.0
0.2
0.4
0.6
0.8
1.0
8.0e+06
1.0e+07
1.2e+07
1.4e+07
Position on scaffold GL429776
Pennsylvania Pre–WNS
Pennsylvania Post–WNS
New York Pre–WNS
New York Post–WNS

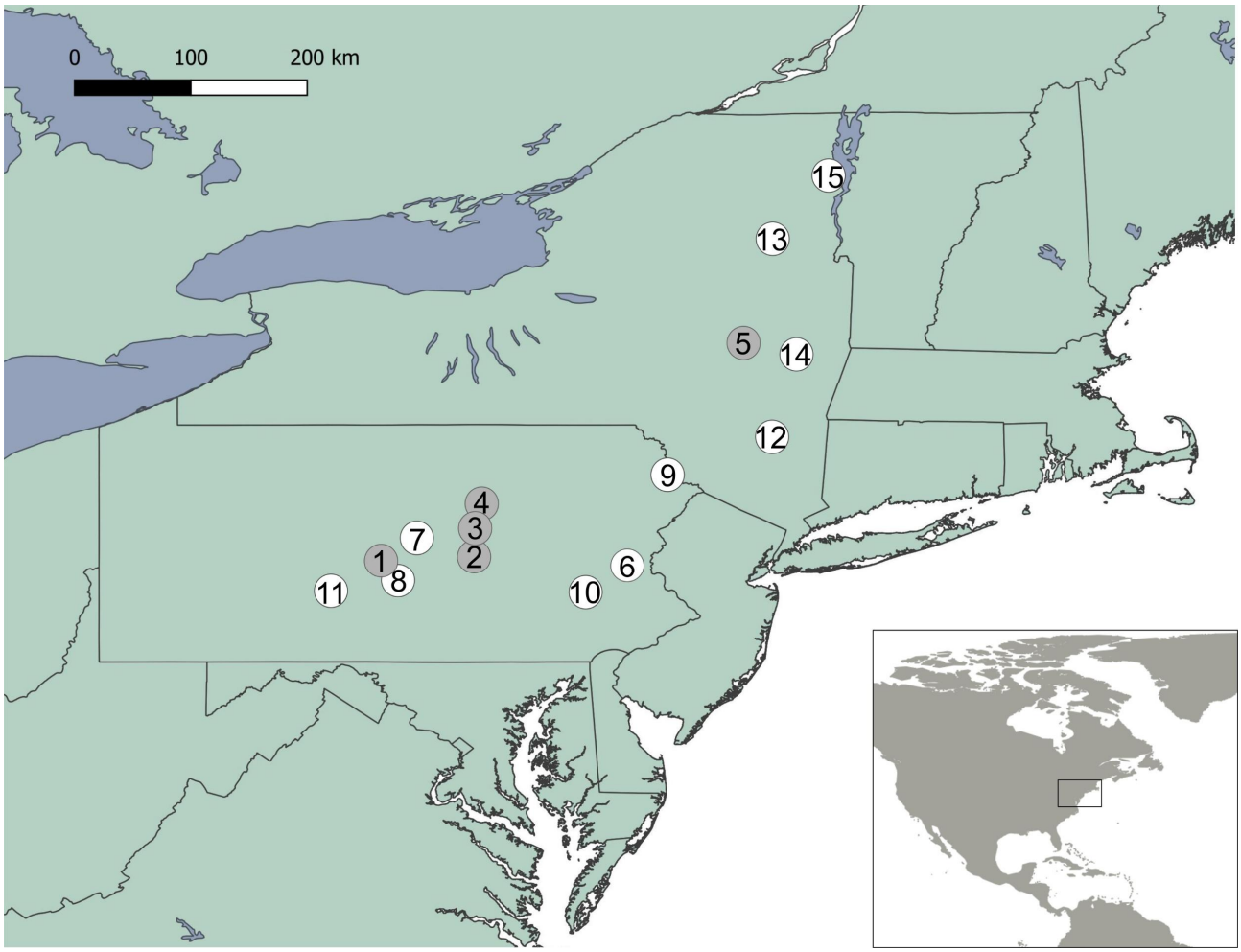
0
100
200 km
15
13
5
14
12
9
4
3
7
2
1
6
8
11
10

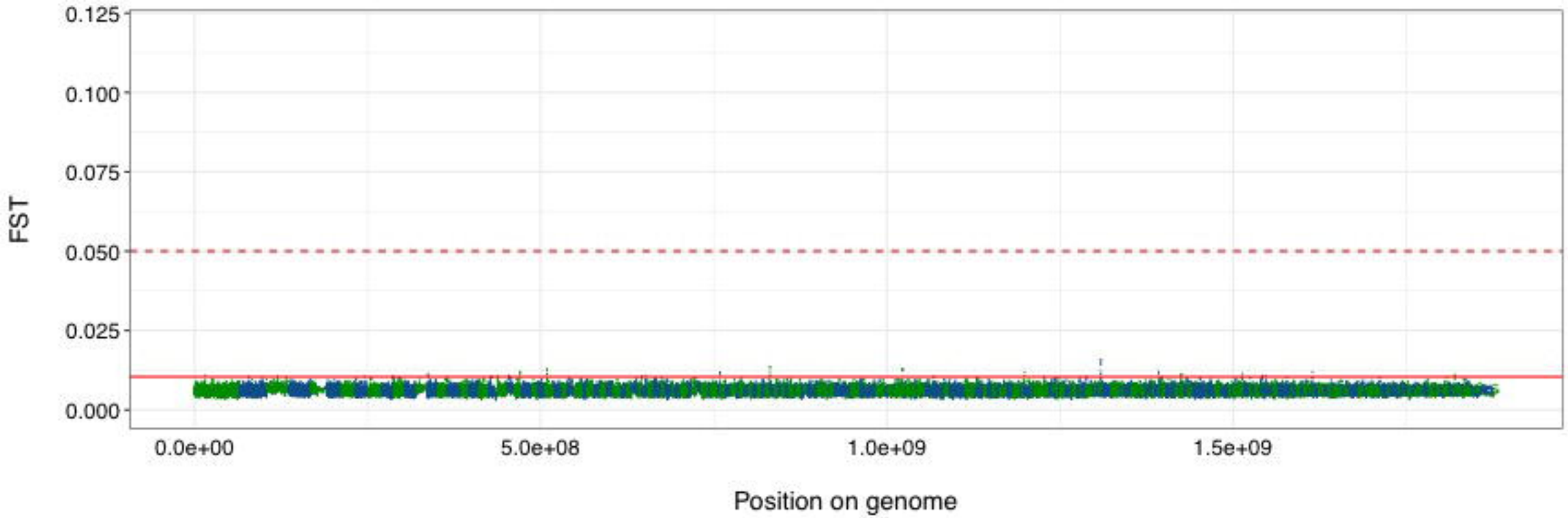
0.125
0.100
0.075
0.050
0.025
0.000
FST
0.0e+00
5.0e+08
1.0e+09
1.5e+09
Position on genome

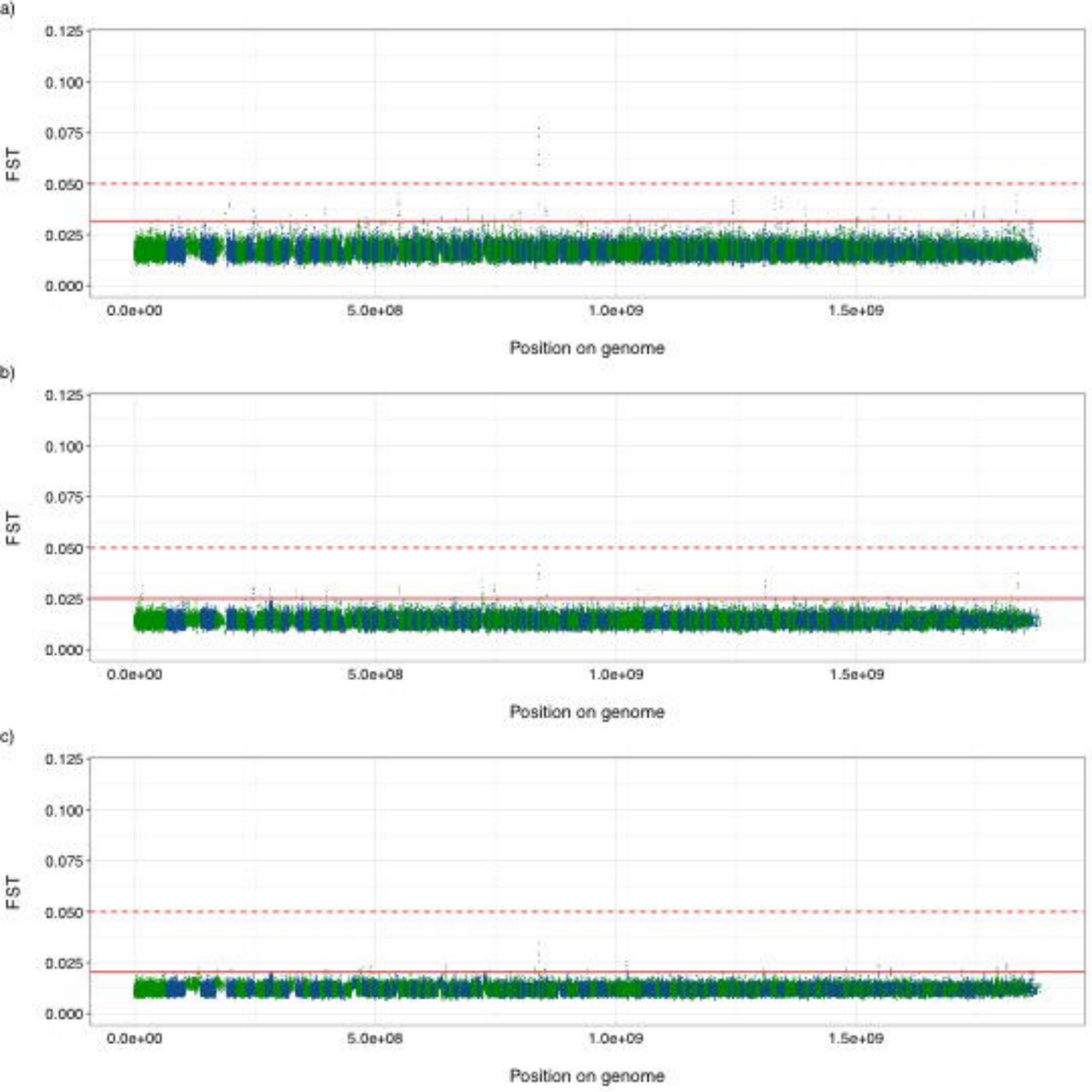
a)
FST
0.125
0.100
0.075
0.050
0.025
0.000
0.0e+00
5.0e+08
1.0e+09
1.5e+09
Position on genome
b)
FST
0.125
0.100
0.075
0.050
0.025
0.000
0.0e+00
5.0e+08
1.0e+09
1.5e+09
Position on genome
c)
FST
0.125
0.100
0.075
0.050
0.025
0.000
0.0e+00
5.0e+08
1.0e+09
1.5e+09
Position on genome

a)

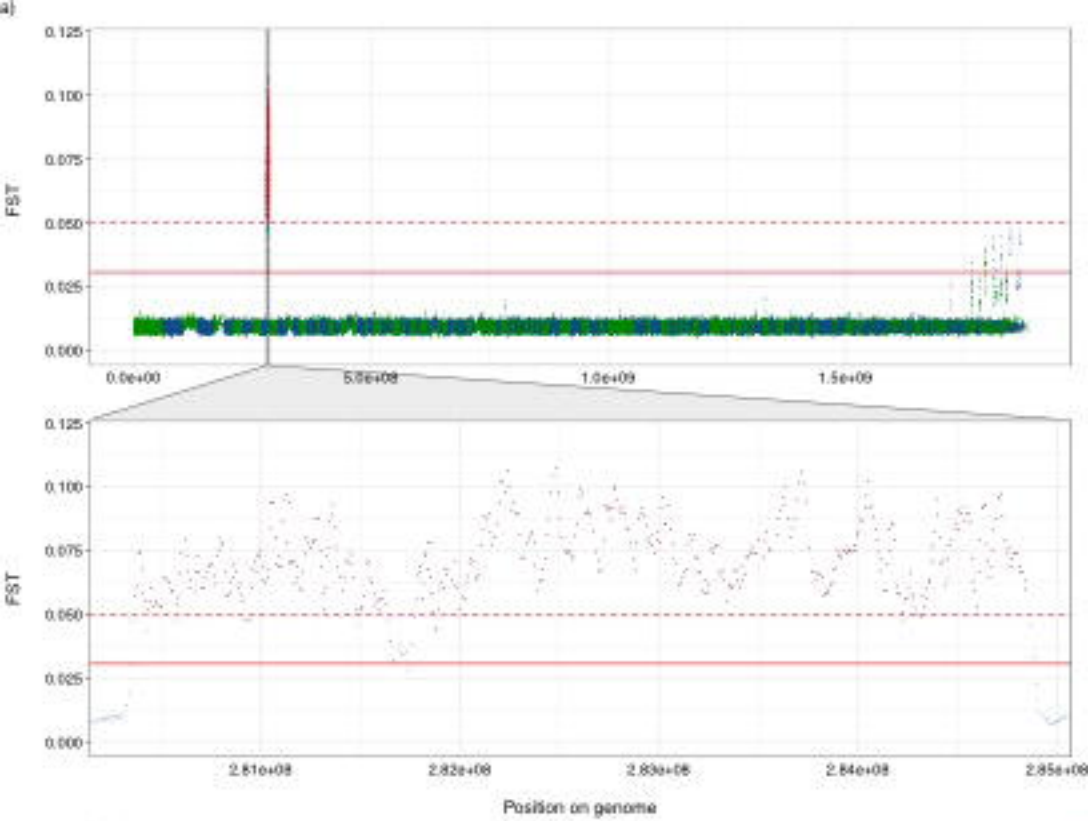
FST
0.125
0.100
0.075
0.050
0.025
0.000
0.0e+00
5.0e+08
1.0e+09
1.5e+09
2.81e+08
2.82e+08
2.83e+08
2.84e+08
2.85e+08
Position on genome
MGAT4C
CUNH12orf50
CEP290
LOC111824948
KITLG
LOC111824954
ATP2B1
POC1B
LOC111824955
CUNH12orf29
TMTC3
LOC111824949
DUSP56

b)

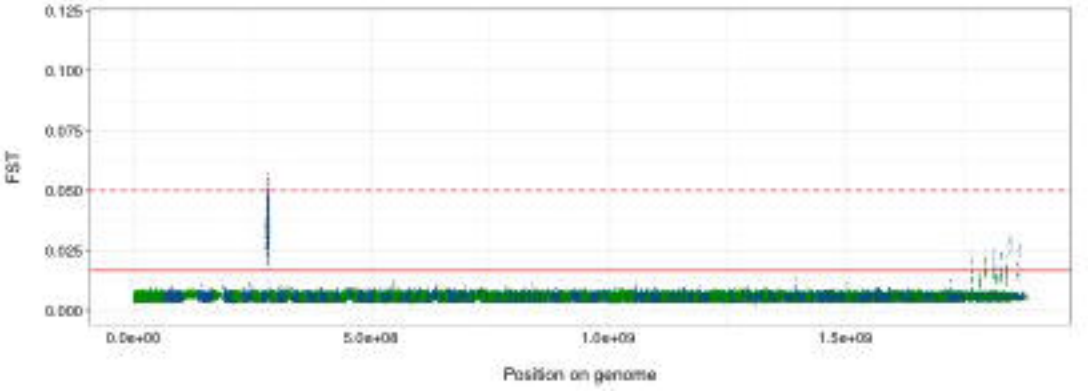
FST
0.125
0.100
0.075
0.050
0.025
0.000
0.0e+00
5.0e+08
1.0e+09
1.5e+09
Position on genome

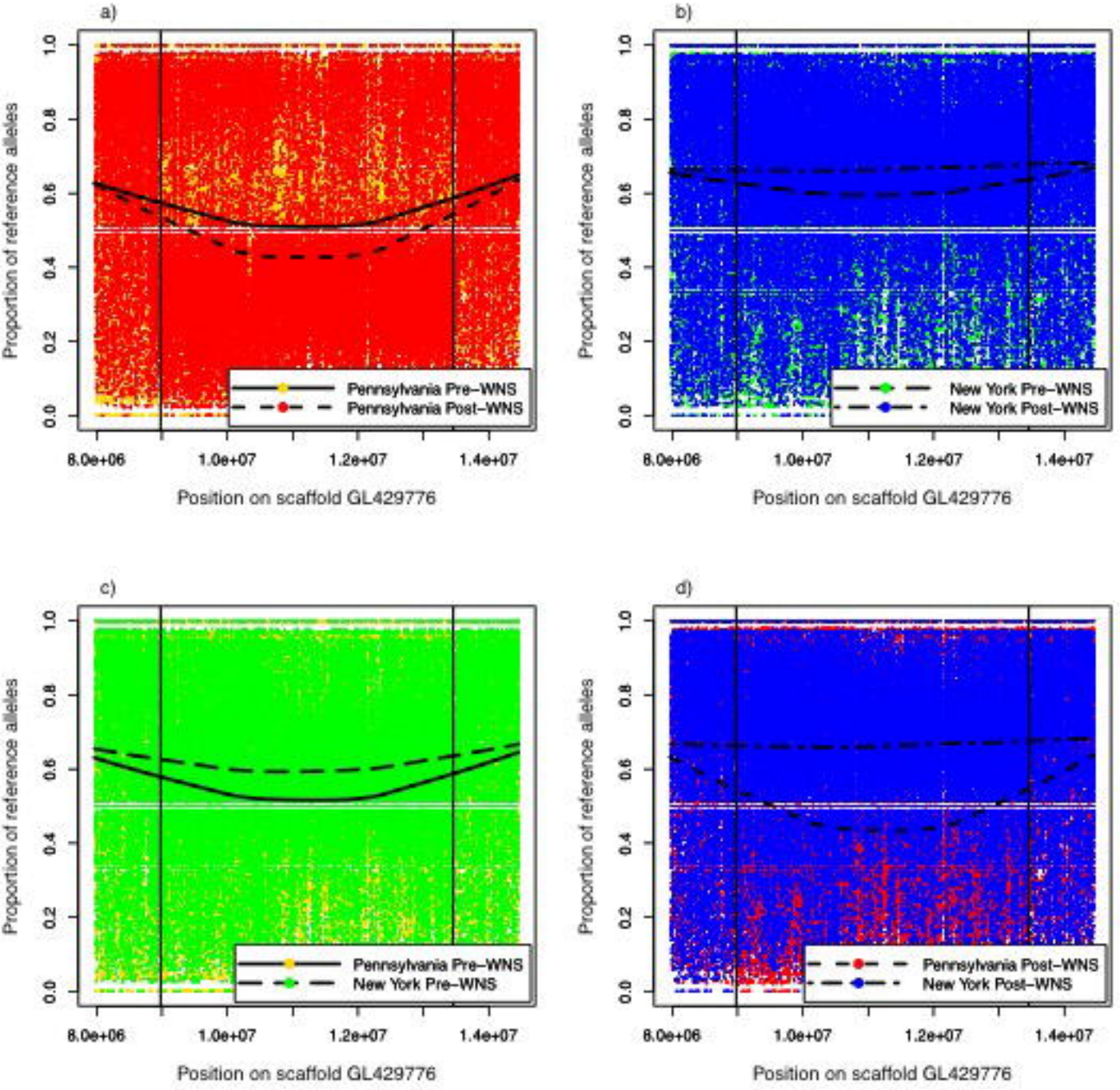
a)
b)
c)
d)
Proportion of reference alleles
0.0
0.2
0.4
0.6
0.8
1.0
8.0e+06
1.0e+07
1.2e+07
1.4e+07
Position on scaffold GL429776
Pennsylvania Pre–WNS
Pennsylvania Post–WNS
New York Pre–WNS
New York Post–WNS